

Discovery of Orally Active Carboxylic Acid Derivatives of 2-Phenyl-5-trifluoromethyloxazole-4-carboxamide as Potent Diacylglycerol Acyltransferase-1 Inhibitors for the Potential Treatment of Obesity and Diabetes

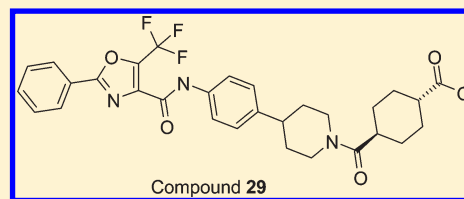
Yimin Qian,^{*,†} Stanley J. Wertheimer,[‡] Mushtaq Ahmad,[†] Adrian Wai-Hing Cheung,[†] Fariborz Firooznia,[†] Matthew M. Hamilton,[†] Stuart Hayden,[†] Shiming Li,[†] Nicholas Marcopulos,[†] Lee McDermott,[†] Jenny Tan,[†] Weiya Yun,[†] Liang Guo,[‡] Anjula Pamidimukkala,[§] Yingsi Chen,^{||} Kuo-Sen Huang,^{||} Gwendolyn B. Ramsey,[⊥] Toni Whittard,[⊥] Karin Conde-Knape,[⊥] Rebecca Taub,[#] Cristina M. Rondinone,[⊥] Jefferson Tilley,[†] and David Bolin[†]

[†]Department of Discovery Chemistry, [‡]Non-Clinical Drug Safety, [§]Metabolism and Pharmacokinetics, ^{||}Discovery Technologies, and [⊥]Metabolic and Vascular Diseases, Hoffmann-La Roche Inc., 340 Kingsland Street, Nutley, New Jersey 07110, United States

[#]Via Pharmaceuticals, Inc., 101 College Road East, Princeton, New Jersey 08540, United States

S Supporting Information

ABSTRACT: Diacylglycerol acyltransferase-1 (DGAT-1) is the enzyme that catalyzes the final and committed step of triglyceride formation, namely, the acylation of diacylglycerol with acyl coenzyme A. DGAT-1 deficient mice demonstrate resistance to weight gain on high fat diet, improved insulin sensitivity, and reduced liver triglyceride content. Inhibition of DGAT-1 thus represents a potential novel approach for the treatment of obesity, dyslipidemia, and metabolic syndrome. In this communication, we report the identification of the lead structure **6** and our lead optimization efforts culminating in the discovery of potent, selective, and orally efficacious carboxylic acid derivatives of 2-phenyl-5-trifluoromethyloxazole-4-carboxamides. In particular, compound **29** (DGAT-1 enzyme assay, $IC_{50} = 57$ nM; CHO-K1 cell triglyceride formation assay, $EC_{50} = 0.5$ μ M) demonstrated dose dependent inhibition of weight gain in diet induced obese (DIO) rats (0.3, 1, and 3 mg/kg, PO, qd) during a 21-day efficacy study. Furthermore, compound **29** demonstrated improved glucose tolerance determined by an oral glucose tolerance test (OGTT).



INTRODUCTION

Triglycerides constitute the major form of energy storage in eukaryotic organisms. In humans, excessive triglyceride accumulation is often associated with diseases such as obesity, diabetes, and steatohepatitis. The key enzyme catalyzing triglyceride synthesis is diacylglycerol *O*-acyltransferase (DGAT). Two DGAT isozymes, DGAT-1 and DGAT-2, each encoded by a distinct gene family, play important roles in triglyceride synthesis.^{1–3} The exact roles played by DGAT-1 and DGAT-2 in triglyceride synthesis are currently under investigation. DGAT-1 deficient mice are resistant to diet induced obesity and have decreased adiposity, in part through increased energy expenditure.⁴ In addition, DGAT-1 null mice are reported with improved insulin and leptin sensitivity.⁵ On the other hand, mice lacking DGAT-2 are lipopenic and die soon after birth.⁶ More recently it was reported that DGAT-1 deficient mice with expression of DGAT-1 only in the intestine completely reversed the resistance to diet induced obesity and hepatic steatosis, which suggested that the beneficial effects of DGAT-1 inhibition might be mainly due to inhibition of the enzyme in the intestine.⁷ Encouraged by the results from DGAT-1^{-/-} mice, we and others

believe that inhibiting DGAT-1 might represent a novel approach for the treatment of obesity and the improvement of insulin sensitivity.^{8,9}

The rapid progress in the search for DGAT-1 inhibitors over the past decade is reflected by the large number of potent compounds disclosed in both the patent and peer reviewed literature.^{10–15} Many of the reported compounds are carboxylic acids, and typical structures are listed in Figure 1. Compound **1** was reported as a potent DGAT-1 inhibitor ($IC_{50} = 44$ nM) and showed efficacy in reducing body weight gain in diet induced obese C57BL/6 mice.¹⁰ Compounds **2** and **3** are examples of DGAT-1 inhibitors disclosed in patent applications from Bayer and Japan Tobacco/Angen, respectively.^{11,12} Compound **3** was recently shown to be efficacious in a mouse DIO model.¹² Compound **4** was reported to be a potent DGAT-1 inhibitor ($IC_{50} = 7$ nM) with oral efficacy by an Abbott research team.¹³ On the basis of lead structure **3**, an AstraZeneca research team reported orally efficacious

Received: December 13, 2010

Published: March 17, 2011

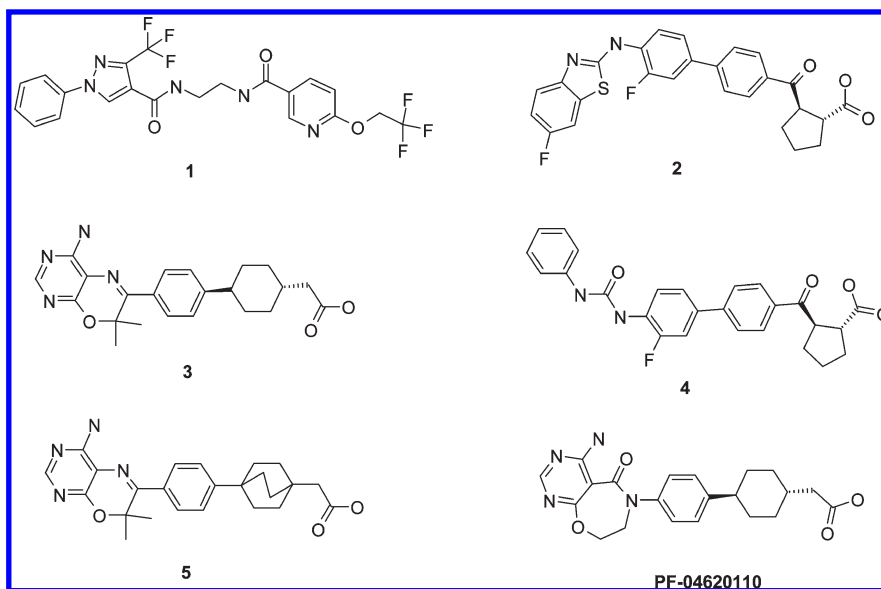


Figure 1. Selected examples of DGAT-1 inhibitors from the literature.

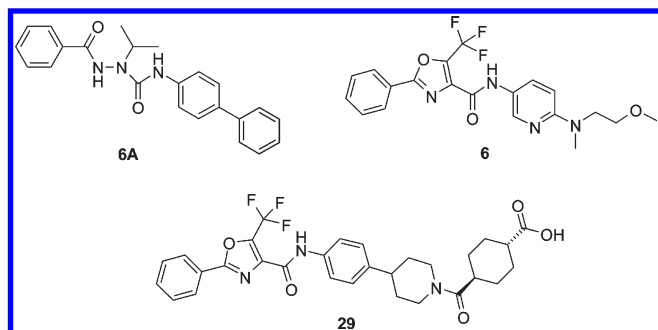


Figure 2. DGAT-1 inhibitor hit molecule **6A**, lead structure **6**, and optimized compound **29**.

pyrimidinoxazinylbicyclooctaneacetic acid derivative **5**.¹⁴ Recently, scientists from Pfizer disclosed PF-04620110 as a development candidate.¹⁵

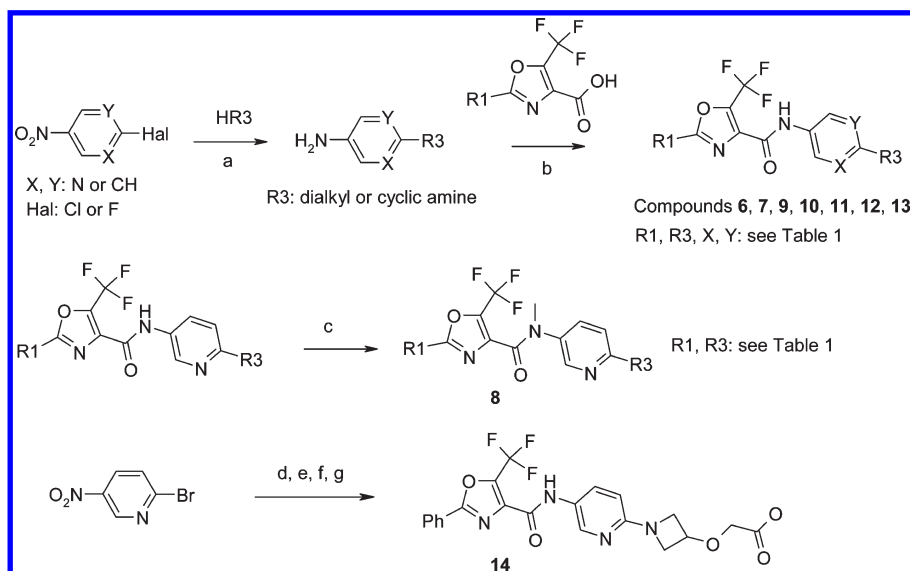
Through the screening of our compound library, we identified a series of hydrazides as DGAT-1 inhibitors. The screening hit **6A** (Figure 2) showed good potency in DGAT-1 enzyme assay ($IC_{50} = 230$ nM). However, the high clearance of this class of hydrazides in vivo prompted us to investigate further structural modifications.¹⁶ During the lead identification process, we replaced the hydrazide moiety with heterocycles and discovered a series of 2-phenyl-5-trifluoromethyloxazole-4-carboxamides as potent DGAT-1 inhibitors.¹⁶ In particular, when assayed for human DGAT-1 enzyme inhibition (potency expressed as IC_{50}) and human DGAT-1 inhibition in CHOK1 cells (potency expressed as EC_{50}), compound **6** ($IC_{50} = 38$ nM, $EC_{50} = 0.66$ μ M, >100-fold selectivity over DGAT-2 and ACAT) emerged as a promising lead and showed desirable pharmacokinetic properties in rats ($CL = 13.5$ mL/min/kg, *iv* at 5 mg/kg) with good oral bioavailability ($F = 77\%$). When dosed orally in DIO rats for 3 weeks, **6** demonstrated good efficacy in reducing body weight gain (4.3% of body weight gain reduction at 25 mg/kg, *po*, *q. d.*).¹⁷ Unfortunately, compound **6** was also shown to block the human ether-a-go-go-related gene (hERG) encoded potassium channel ($IC_{20} = 0.2$ μ M), and further assessment in the guinea

pig Langendorff heart model indicated that **6** induced dispersion of repolarization and caused QT prolongation at low concentrations consistent with the in vitro hERG data. In light of these results, our lead optimization strategy focused on maintaining DGAT-1 enzyme and cellular inhibition potency while reducing the hERG channel interaction. In addition to resolving hERG issues, we also sought to further improve the pharmacokinetic properties of **6** to achieve efficacy at lower doses. Since carboxylic acids are rarely associated with hERG liabilities,¹⁸ we investigated the effects of incorporation of carboxylic acid moieties into our lead structure. This strategy led to elimination of the hERG inhibition while maintaining both in vitro and in vivo potency. Herein we report the details of this work and the identification of the orally active and potent DGAT-1 inhibitor **29**, with improved pharmacokinetic properties and significantly decreased hERG liabilities.

CHEMISTRY

Compounds **6–14** were prepared as described in Scheme 1. The commercially available 2-phenyl-5-trifluoromethyloxazole-4-carboxylic acid or 2-methyl-5-trifluoromethyloxazole-4-carboxylic acid were coupled with the appropriate aromatic or heteroaromatic amines in the presence of bromotripyrrolidino-phosphonium hexafluorophosphate. The heteroaromatic amines were in turn synthesized by the S_NAr reaction of halogen-substituted nitroaromatics with amines, followed by the reduction of the nitro group (Scheme 1).

To prepare amides and carbamates **15–24**, the substituted piperidine or piperazine hydrochlorides (**31**, **32**, **33**, **34**, and **35**) were used as the key intermediates. The hydrochloride salt **31** was prepared through the amide coupling reaction of 2-phenyl-5-trifluoromethyloxazole-4-carboxylic acid with the corresponding amine followed by the deprotection of the *tert*-butoxycarbonyl group (Scheme 2). Intermediates **32**, **33**, and **34** were prepared via a similar method (see the Experimental Section). For the synthesis of intermediate **35**, 2-bromo-5-nitropyridine was first coupled with the pinacolboronate of *N*-Boc-tetrahydropyridine under Suzuki coupling conditions, followed by hydrogenation

Scheme 1. Preparation of Compounds 6–14^a

^a Reaction conditions: (a) (i) triethylamine, THF, room temp or heat; (ii) H₂ (50 psi), Pd/C (cat.), THF/MeOH; (b) PyBroP, triethylamine, DMF; (c) methyl iodide, NaH, DMF; (d) azetidin-3-ol hydrochloride, K₂CO₃, NMP, heat; (e) (i) bromoacetic acid *tert*-butyl ester, NaH, THF/DMF; (ii) H₂ (50 psi), Pd/C (cat.); (f) 2-phenyl-5-trifluoromethyloxazole-4-carboxylic acid, PyBroP, DMF; (g) CF₃COOH, CH₂Cl₂.

and subsequent amide coupling reaction (Scheme 2). Treatment of the intermediates 31–35 with the appropriate acyl chloride or alkoxycarbonyl chlorides afforded compounds 15–24.

The synthesis of *trans*-1,4-cyclohexane carboxylic acid derivatives is illustrated in Scheme 3. The intermediates required for the preparation of compounds 25–30, namely, *trans*- and *cis*-1,4-cyclohexane dicarboxylic acid monobenzyl ester, were synthesized through monoacyl chloride formation and quenching with benzyl alcohol (Scheme 3).

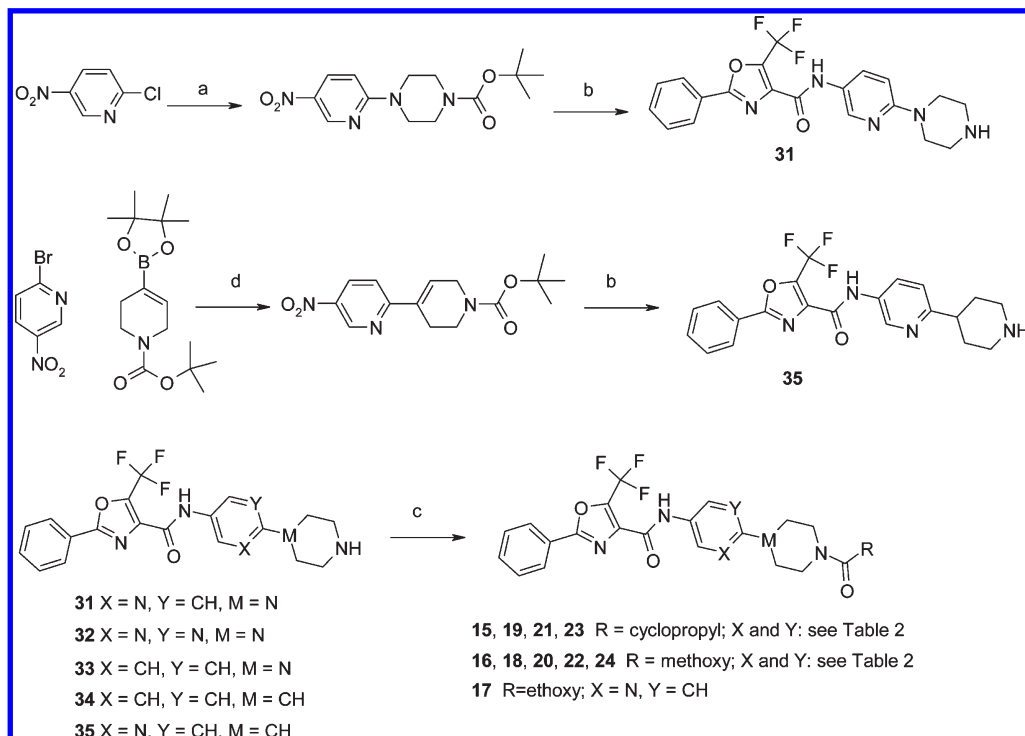
RESULTS AND DISCUSSION

Compounds prepared in the present work (6–30) were assayed for human DGAT-1 enzyme inhibition (expressed as IC₅₀), human DGAT-1 inhibition in CHOK1 cells (expressed as EC₅₀), and hERG channel inhibition (expressed as IC₂₀). As shown in Table 1, 6 displayed significant hERG inhibition despite the lack of a basic amine in the structure. Since hERG inhibition can induce torsade de pointes (TdP) in human,^{19,20} prevention of hERG potassium channel blocking has thus been adopted as a routine drug toxicity derisking strategy. To overcome the hERG blocking issue, we first looked at the structural fragments in compound 6 with the goal of understanding their contributions to hERG channel inhibition. The results are summarized in Table 1 below.

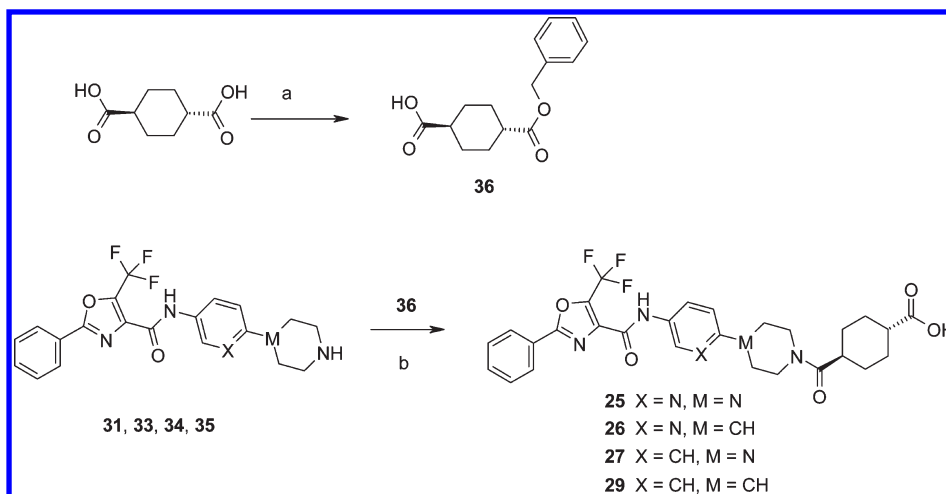
The above results from compounds 6–10 indicated that multiple factors contributed to hERG inhibition. Changing the pyridine moiety in 6 to pyrimidine or benzene slightly decreased hERG inhibition (compounds 9 and 10 compared to 6), while cyclization of *N*-methyl-*N*-methoxyethylamine A to azetidine B (compound 11) did not affect hERG inhibition significantly. Interestingly, reducing the basicity of the nitrogen of the R3 by placing fluorine atoms in the β position (compound 13) did not have any significant impact on hERG inhibition either. To our surprise, increased DGAT-1 inhibition in compound 13 was accompanied by a loss in cellular activity, possibly due to the poor

solubility (mp 217 °C, solubility of <1 μg/mL). On the other hand, increasing the polarity significantly reduced hERG channel interaction (compound 12), albeit accompanied by a 6-fold loss of DGAT-1 inhibition potency relative to 6. Significant improvements in hERG liability came from amide methylation or R1 substitution (compounds 7 and 8), which may be explained by a conformational change or an increase in polarity. Unfortunately, both compounds 7 and 8 lost DGAT-1 potency. Finally, the incorporation of a carboxylic acid almost completely alleviated hERG blockade despite a modest loss of DGAT-1 enzyme inhibition (compound 14). This result is consistent with the observation that the hERG channel tends to bind strongly with positively charged molecules such as tertiary amines. The loss of cellular potency in compound 14 was presumably due to its poor cell permeability (cpKa = 2.9, log *D* = −0.20).

Although we were able to decrease hERG inhibition by adding a carboxylic acid moiety (compound 14), the same carboxylic acid group also resulted in a loss of DGAT-1 cellular activity. We next extended our investigation of the R3 substitution in order to improve DGAT-1 potency. The results are summarized in Table 2. Rigidification of the R3 substitution through the incorporation of a piperazine or a piperidine moiety and capping the distal nitrogens as amides or carbamates all resulted in potent DGAT-1 inhibition in both enzyme and cellular assays (compounds 15–24, Table 2). When compared to 6, compound 17 demonstrated 6-fold potency improvement in the DGAT-1 cellular assay and a 4-fold reduction in hERG channel activity. With the exception of compound 15, all piperazine/piperidine derivatives (16–24) demonstrated reduced hERG inhibition. Of particular interest were compounds 23 and 24, which displayed the most significant improvement in hERG inhibition. However, when 23 and 24 were further evaluated in mice, they both displayed very low oral exposure after dosing as an aqueous suspension to DIO mice at 25 mg/kg, with compound 23 showing plasma C_{max} of 76 ng/mL at T_{max} of 1 h and compound 24 showing C_{max} < 10 ng/mL.

Scheme 2. Preparation of Piperazine/Piperidine Substituted Amides and Carbamates^a

^a Reaction conditions: (a) *N*-Boc-piperazine, potassium carbonate, acetonitrile, 80 °C; (b) (i) H₂ (50 psi), Pd/C (cat.), THF/MeOH; (ii) 2-phenyl-5-trifluoromethyloxazole-4-carboxylic acid, PyBroP, triethylamine, DMF; (iii) HCl in ether, CH₂Cl₂, MeOH; (c) cyclopropylcarbonyl chloride or methoxycarbonyl chloride or ethoxycarbonyl chloride, triethylamine, CH₂Cl₂; (d) PdCl₂dppf (cat.), potassium carbonate, toluene/ethanol, 100 °C, microwave.

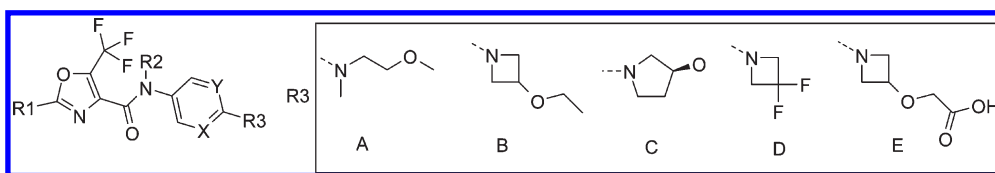
Scheme 3. Synthesis of *trans*-1,4-Cyclohexane Carboxylic Acid Derivatives^a

^a Reaction conditions: (a) (i) oxalyl chloride, cat. DMF, THF; (ii) benzyl alcohol, THF; (b) (i) oxalyl chloride, CH₂Cl₂; (ii) Et₃N, CH₂Cl₂; (iii) H₂, Pd/C, MeOH/THF

Therefore, to improve the pharmacokinetic properties of compound **24** while maintaining potent DGAT-1 inhibition in enzyme and cellular assays, we derivatized the piperazine/piperidine groups with six-membered rings functionalized with carboxylic acids. Results from these modifications are summarized in Table 3. Only compounds with good potency in DGAT-1

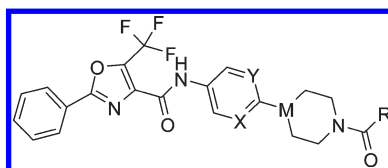
enzyme and cellular assays (IC₅₀ < 0.5 μM or EC₅₀ < 1.0 μM) were tested for hERG channel inhibition.

As illustrated in Table 3, incorporation of a carboxylic acid significantly reduced hERG channel inhibition. When compared to neutral compounds (Table 2), carboxylic acid derivatives showed reduced cellular activity (compare **17** with **25**).

Table 1. Substitution Effects on DGAT-1 Activity and hERG Inhibition^a

compd	R1	R2	R3	X	Y	DGAT-1 IC ₅₀ (μM)	DGAT-1 EC ₅₀ (μM)	hERG IC ₂₀ (μM) or % inhibition at x (μM)
6	phenyl	H	A	N	CH	0.038	0.661	0.2
7	methyl	H	A	N	CH	15.1	>25	37% at 30
8	phenyl	methyl	A	N	CH	24.7	>25	34% at 30
9	phenyl	H	A	N	N	0.048	0.534	1.5
10	phenyl	H	A	CH	CH	0.325	1.803	18% at 1
11	phenyl	H	B	N	CH	0.068	0.228	0.37
12	phenyl	H	C	N	N	0.237	5.66	10.0
13	phenyl	H	D	N	CH	0.016	25.0	17% at 1
14	phenyl	H	E	N	CH	0.202	>25	12% at 30

^a Mean values from at least three experiments.

Table 2. Structure–Activity Relationships of Substituted Piperazine and Piperidine^a

compd	X	Y	M	R	DGAT-1 IC ₅₀ (μM)	DGAT-1 EC ₅₀ (μM)	hERG IC ₂₀ (μM) or % inhibition at x (μM)
15	N	CH	N	cyclopropyl	0.059	0.138	0.18
16	N	CH	N	methoxy	0.028	0.216	1.94
17	N	CH	N	ethoxy	0.041	0.093	0.80
18	N	N	N	methoxy	0.071	0.41	28% at 1.0
19	N	CH	CH	cyclopropyl	0.128	0.378	1.73
20	N	CH	CH	methoxy	0.084	0.219	16% at 1.0
21	CH	CH	N	cyclopropyl	0.136	0.165	35% at 3.0
22	CH	CH	N	methoxy	0.165	0.190	16% @ 3.0
23	CH	CH	CH	cyclopropyl	0.067	0.362	13% at 3.0
24	CH	CH	CH	methoxy	0.084	0.371	41% at 30.0

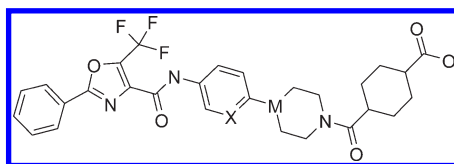
^a Mean values from at least three experiments.

Incorporation of heteroaromatics such as pyridine into the structures also led to reduced cellular potency (compare **26** with **29**), possibly due to the lowered hydrophobicity (compound **29** clogP = 3.1, compound **26** clogP = 1.9). The literature carboxylic acid **3** displayed similar difference between enzyme and cellular potency in our assay despite its higher lipophilicity (clogP = 4.6). Of these analogues, **29** exhibited the best combination of cellular potency in the DGAT assay and minimal hERG liability.

Thus, compound **29** was selected for further investigation. When assayed for its selectivity toward human DGAT-1 over human DGAT-2 (IC₅₀ > 100 μM) and ACAT (a mixture of ACAT1 and ACAT2, IC₅₀ = 68.4 μM), it showed over 4000-fold and 2000-fold selectivity, respectively. When assayed for rat

DGAT-1 inhibition, it showed comparable potency to human DGAT-1. Compound **29** also displayed desirable physicochemical properties (solubility of 15.4 μg/mL; log D = 2.34; pK_a = 5.78; caco-2 permeability of 245 × 10⁻⁷ cm/s; free fraction in human serum protein binding of 0.7%; human hepatocyte clearance of 3.14 (mL/min)/kg; rat hepatocyte clearance of 5.77 (mL/min)/kg; P450 inhibition for CYP2C9, 2C19, 2D6, and 3A4, IC₅₀ > 50 μM, no CYP3A4 time dependent inactivation and no P-glycoprotein inhibition).

We next determined the pharmacokinetic (PK) profiles of **29** in rats and dogs. The PK results are summarized in Table 4. As observed with other carboxylic acids in this class of molecules, compound **29** has a low volume of distribution and low clearance.

Table 3. DGAT-1 and hERG Inhibition Potency of Cyclohexane 1,4-Dicarboxylic Acid Derivatives^a

compd	X	M	cis or trans	DGAT-1 IC ₅₀ (μM)	DGAT-1 EC ₅₀ (μM)	hERG IC ₂₀ (μM) or % inhibition at x (μM)
25	N	N	trans	0.035	1.764	ND
26	N	CH	trans	0.128	2.363	ND
27	CH	N	trans	0.277	1.070	5% at 1.0
28	CH	N	cis	0.077	0.365	>10
29	CH	CH	trans	0.057	0.493	30.0
30	CH	CH	cis	0.082	0.220	21% at 3.0
3				0.113	1.436	ND

^a Mean value from at least three experiments. ND: not determined.

Table 4. Pharmacokinetic (PK) Properties of Compound 29 in Rat and Dog^a

PK parameter	rat	dog
iv dose (mg/kg)	5	5
Vd (L/kg)	0.27	0.38
CL ((mL/min)/kg)	0.38	1.3
T _{1/2} (h)	8.6	5.3
po dose (mg/kg)	10	10
AUC _{ext} (μM·h)	566.8	77.9
C _{max} (μM)	34.8	4.7
T _{max} (h)	12	2
F (%)	73	33

^a All numbers are the mean average ($n = 3$).

The observed low clearance could be due to the high microsomal stability and high protein binding. Interestingly, when the corresponding cis-isomer compound 30 was orally dosed in mice, both the cis-isomer and the trans-isomer compound 29 were detected in plasma in an almost 1:1 ratio resulting from isomerization. On the other hand, when the trans-isomer was dosed in mice, no in vivo isomerization was observed.

On the basis of its desirable pharmacokinetic properties, compound 29 was selected for 1 week efficacy screening in male DIO rats. When dosed at 3 mg/kg (po, q.d.), it caused a significant reduction (4.0%) in body weight gain. At the end of the study, rats were challenged with corn oil (4 h fast, 5 mL/kg), and a reduction of plasma triglyceride levels by 85% was observed at the 4 h time point compared to the vehicle-treated group ($p = 0.015$). Encouraged by these data, we initiated studies aimed at determining the dose response of 29 on decreasing body weight gain in DIO rats in a more chronic setting. Therefore, compound 29 was orally dosed at 0.3, 1.0, and 3.0 mg/kg once a day for 3 weeks. As shown in Figure 3, rats in the vehicle-treated group fed a high fat diet for 3 weeks gained significant weight. However, in rats treated with 29, we observed a dose dependent decrease in body weight gain (by 5%, 6%, and 8% at doses of 0.3, 1.0, and 3.0 mg/kg, respectively, $p < 0.01$). This dose dependent efficacy correlated well with the measured exposure levels (C_{max} of 2.0, 4.8, and 15.1 μM at doses of 0.3, 1.0, and 3.0 mg/kg, respectively).

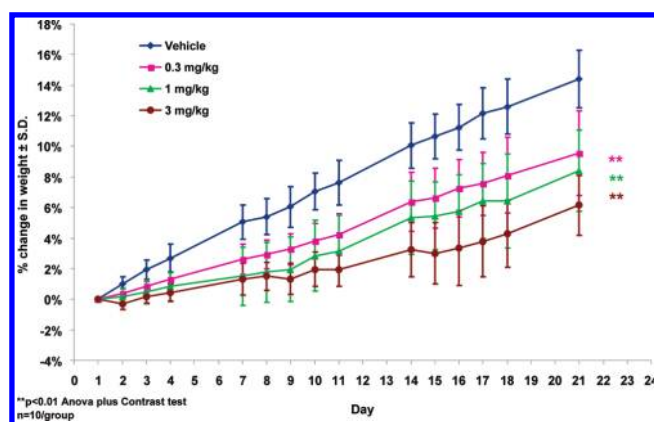


Figure 3. Effects of compound 29 on body weight change of DIO rats (orally dosed at 0.3, 1, and 3 mg/kg) for 3 weeks.

We also measured daily food intake on days 1–3, 8, 9, 15, and 16. As shown in Figure 4, treatment with 29 for 3 weeks caused a dose dependent decrease in food intake (17%, 19%, and 27% at doses of 0.3, 1, and 3 mg/kg, respectively, $p < 0.01$). These data suggested that part of the effect of compound 29 on body weight may be due to reduced food intake.

To further investigate the potential beneficial effects of compound 29 on glucose homeostasis, an oral glucose tolerance test (OGTT) was carried out on DIO rats on the last day of the 3-week efficacy studies. Our data indicated that 29 significantly lowered the overall glucose excursion by 15% at a dose of 3 mg/kg (Figure 5). Although lower doses (0.3 and 1 mg/kg) also showed trends in lowering glucose excursion, data analysis suggested that they did not reach significance. We also measured insulin levels on day 21 prior to OGTT and compared them with the insulin levels measured on day 1 prior to the treatment by compound 29. Our data indicated a significant decrease in basal insulin levels after DIO rats were treated with compound 29 (3 mg/kg, data in Supporting Information), while the basal glucose level was comparable to that of the vehicle group (Figure 5). When insulin levels were measured at the 30 min time point during OGTT, we did not observe significant changes in insulin levels between the vehicle group and the groups treated with 29

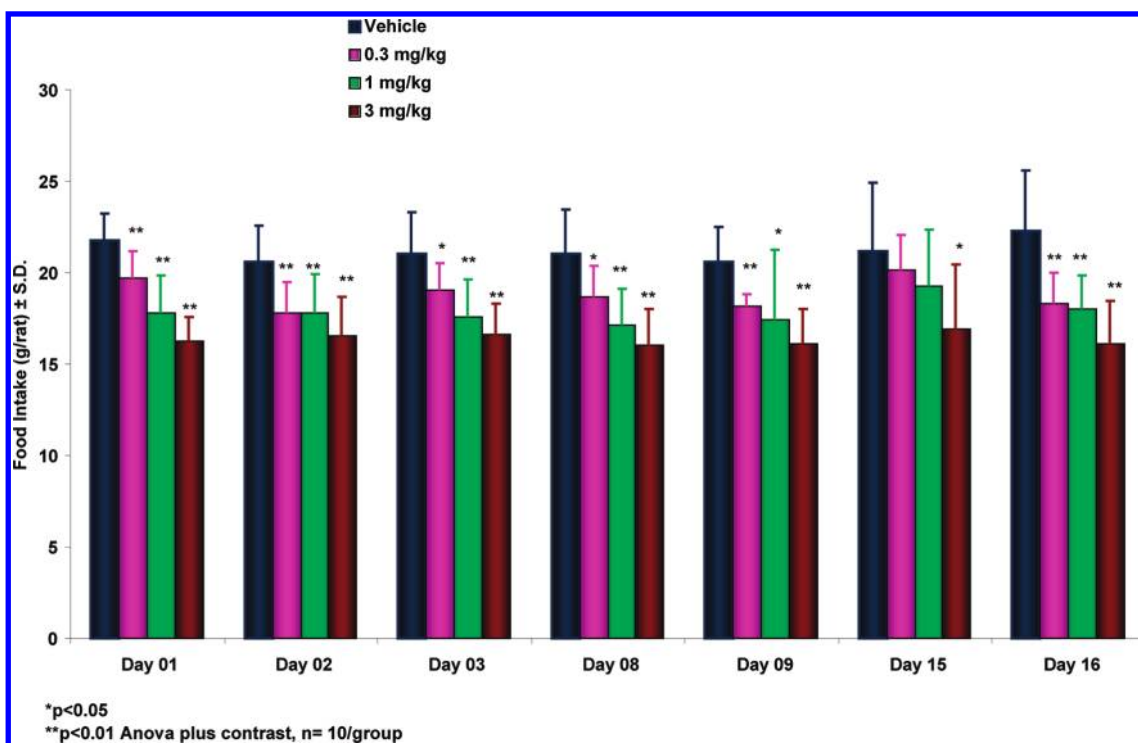


Figure 4. Measured food intake in DIO rats dosed with compound **29** (0.3, 1, and 3 mg/kg). All measurements are daily food intake (10 rats per dose group). Values are the average for each group.

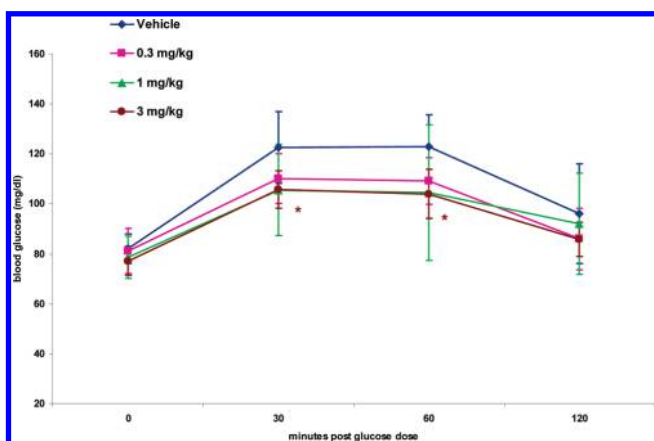


Figure 5. Effects of compound **29** on oral glucose tolerance test (OGTT). Glucose was measured at 0, 30, 60, and 120 min after oral glucose treatment at 2 g/kg (10 rats each dose group). All numbers are the average: (*) $p < 0.05$ for glucose AUC, Anova contrast test.

at the three doses. However, the glucose level was significantly lower for the group treated with **29** (3 mg/kg, Figure 5). These data suggested a potential insulin sensitizing effect of compound **29** in DIO rats. The encouraging OGTT result in terms of reduced glucose excursion in addition to the effects on insulin levels and on lowering body weight gain suggested that DGAT-1 inhibitor **29** could provide potential benefits for treating obesity and diabetes.

Since the publication of mouse DGAT-1^{-/-} data, significant efforts have been carried out in the industry to identify potent small molecule DGAT-1 inhibitors.⁸ In our studies, the reduction of body weight gain in DIO rats by a selective DGAT-1 inhibitor

was accompanied by a reduction in food intake. The exact mechanism of how selective DGAT-1 inhibitors can affect food intake is not clear. One possible explanation is that inhibiting DGAT-1 can affect fatty acid composition, distribution, and sensing mechanisms, which may have an impact on food intake. In fact, it was recently reported that gastric emptying was significantly delayed and incretin hormones GLP-1 and PYY were elevated in DGAT-1 deficient mice compared to the wild type after oral triglyceride loading.²¹ GLP-1 and PYY are intestine incretin hormones that can affect food intake,^{22,23} which could explain the observed anorectic effects of DGAT-1 inhibitors. In our efficacy studies, plasma GLP-1 and PYY were not measured. Further support for a local effect of DGAT in the gut comes from the recent report that DGAT-1 deficient mice with specific expression of DGAT-1 in intestine completely reversed the resistance to diet induced obesity and hepatic steatosis normally associated with DGAT-1 knockout, suggesting that the effects of DGAT-1 on body weight gain are largely contributed by the inhibition of the enzyme in the intestine.⁷ The effects of DGAT inhibition on food intake in rats treated with compounds of completely different chemical structures have also been reported in literature.²⁴

To further assess selectivity of compound **29**, a panel of 80 receptors and ion channels were selected for a radiolabeled binding assay (data in Supporting Information). Compound **29** showed a clean profile ($IC_{50} > 10 \mu M$) for 77 out of 80 targets in the panel, including potential targets that can affect food intake and body weight, such as cannabinoid (CB1), cholecystokinin (CCK), dopamine (D2), ghrelin, histamine, serotonin, NPY, nuclear receptor PPAR, and purinergic receptor (PX). The only three targets from the panel that showed strong interactions with compound **29** are the adenosine receptors (A2A and A3) and the dopamine receptor (D3). It is unlikely

that activities at the three receptors in the panel are related to the food intake effects observed with compound **29**, as another very similar carboxylic acid analogue (structure not shown) with a clean profile of binding to A2A, A3, and D3 demonstrated almost identical effects on food intake and body weight in DIO rats. Furthermore, when total brain concentration of compound **29** was measured, it showed brain to plasma ratio of only 3%. We also did not observe any changes regarding locomotor activity, clinical signs, or clinical chemistry in the 3-week efficacy study.

In summary, we have identified a novel class of 2-phenyl-5-trifluoromethyloxazole-4-carboxamides, which demonstrated good in vitro DGAT-1 inhibition and high selectivity for DGAT-1, without affecting the hERG potassium channel. One of the described compounds, **29**, showed good PK properties and significant efficacy in obesity models with beneficial effects on glucose homeostasis. Compound **29** was evaluated in several in vitro toxicity assays (cyp inhibition, protein covalent binding, micronucleus test, and Ames test) and displayed no liabilities. Our results provided further evidence that selective small molecule DGAT-1 inhibitors could have beneficial effects on metabolic syndromes.

EXPERIMENTAL SECTION

All reactions were carried out under an argon atmosphere. All solvents were purchased from commercial sources without further drying. Melting points were taken on a Buchi melting point B-545 apparatus without correction. ^1H NMR spectra were recorded with Mercury 300 and Unityplus 400 MHz spectrometers. The reference peaks are as follows: CDCl_3 δ ppm 7.27, CD_3OD δ ppm 3.31, $\text{DMSO-}d_6$ δ ppm 2.50. All compounds were analyzed by LC/MS (liquid chromatography/mass spectrometry) using Waters ZQ mass detector and Waters LC system. Ionization was generally achieved via electron spray (ES). The LC fraction detection consisted of both diode array detector and evaporative light scattering detector, and all tested compounds had purity greater than 98%. Combustion elemental analysis was applied to compound **29**. Thin layer chromatography was run on silica coated glass plate and was visualized under 254 nm UV or iodine vapor. Preparative high pressure liquid chromatography (HPLC) was carried out using a Rainin HPLC employing a 41.4 mm \times 300 mm, 8 μm , Dynamax C-18 column at a flow of 49 mL/min employing a gradient of acetonitrile/water (each containing 0.75% TFA) typically from 5% to 95% acetonitrile over 35–40 min.

2-Phenyl-5-trifluoromethyloxazole-4-carboxylic Acid {6-[(2-Methoxyethyl)methylamino]pyridin-3-yl}amide (6). To a mixture of 2-chloro-5-nitropyridine (1.58 g, 9.96 mmol) and 2-methoxyethylmethylamine (1.78 g, 20 mmol) in THF (30 mL) was added triethylamine (1.38 mL), and the solution was stirred at room temperature overnight. The resulting mixture was filtered, and the filtrate was evaporated. The residue was extracted with ethyl acetate and water. The organic layer was washed with brine and dried over sodium sulfate. Solvents were evaporated and the residue was dried under vacuum overnight to give pure desired compound 2-methoxyethylmethyl-(5-nitropyridin-2-yl)amine (2.13 g, 100%). This oily material (570 mg, 2.70 mmol) was dissolved in methanol (30 mL), and palladium on carbon (5%, 35 mg) was added. The mixture was hydrogenated at 30 psi for 1 h and then filtered. Solvents were evaporated, and the residue was dried under vacuum overnight. The resulting material was combined with 2-phenyl-5-trifluoromethyloxazole-4-carboxylic acid (694 mg, 2.70 mmol) and bromotripyrrolidino-phosphonium hexafluorophosphate (1.26 g, 2.70 mmol) in DMF (15 mL) containing triethylamine (0.8 mL). The solution was stirred overnight, and solvents were evaporated. The residue was extracted with dichloromethane and water. The organic layer was washed with sodium

bicarbonate solution and dried over sodium sulfate. Solvents were evaporated, and the residue was purified through ISCO flash column chromatography (linear gradient ethyl acetate in hexanes) to give 2-phenyl-5-trifluoromethyloxazole-4-carboxylic acid {6-[(2-methoxyethyl)methylamino]pyridin-3-yl}amide (828 mg, 73%). LC–MS calcd for $\text{C}_{20}\text{H}_{19}\text{F}_3\text{N}_4\text{O}_3$ (*m/e*) 420.14, obsd 421.0 (M + H). ^1H NMR (300 MHz, CDCl_3) δ 8.73 (br s, 1H), 8.24 (br s, 1H), 8.02–8.19 (m, 3H), 7.48–7.65 (m, 3H), 6.54 (d, J = 8.15 Hz, 1H), 3.76 (br s, 2H), 3.60 (br s, 2H), 3.37 (s, 3H), 3.10 (s, 3H).

2-Methyl-5-trifluoromethyloxazole-4-carboxylic Acid {6-[(2-Methoxyethyl)methylamino]pyridin-3-yl}amide (7). N^2 -(2-Methoxy-ethyl)- N^2 -methylpyridine-2,5-diamine (56 mg, 0.309 mmol), 2-methyl-5-trifluoromethyloxazole-4-carboxylic acid (50 mg, 0.256 mmol), and Et_3N (0.198 mL, 0.768 mmol) were treated with BOP (119 mg, 0.268 mmol) in 2 mL of DMF. Following workup, the crude material was purified by flash chromatography to yield 2-methyl-5-trifluoromethyloxazole-4-carboxylic acid {6-[(2-methoxyethyl)methylamino]pyridin-3-yl}amide as a lyophilized powder (28 mg, 30%). LC–MS calcd for $\text{C}_{15}\text{H}_{17}\text{F}_3\text{N}_4\text{O}_3$ (*m/e*) 358.318, obsd 359.2 (M + H). ^1H NMR (300 MHz, $\text{DMSO-}d_6$) δ 10.38 (s, 1H), 8.37 (d, J = 2.6 Hz, 1H), 7.85 (dd, J = 2.6, 9.2 Hz, 1H), 6.60 (d, J = 9.2 Hz, 1H), 3.60–3.69 (m, 2H), 3.42–3.50 (m, 2H), 3.22 (s, 3H), 2.98 (s, 3H), 2.58 (s, 3H).

2-Phenyl-5-trifluoromethyloxazole-4-carboxylic Acid {6-[(2-Methoxyethyl)methylamino]pyridin-3-yl}methylamide (8). 2-Phenyl-5-trifluoromethyloxazole-4-carboxylic acid {6-[(2-methoxyethyl)methylamino]pyridin-3-yl}amide (**6**) (50 mg, 0.119 mmol) was treated with sodium hydride (60% in oil, 10.4 mg, 0.238 mmol) and methyl iodide (22 μL , 0.357 mmol) in 5 mL THF at room temperature for 16 h. Following workup, the crude material was purified by flash chromatography to yield 2-phenyl-5-trifluoromethyloxazole-4-carboxylic acid {6-[(2-methoxyethyl)methylamino]pyridin-3-yl}methylamide as a solid (29 mg, 56%). LC–MS calcd for $\text{C}_{21}\text{H}_{17}\text{F}_3\text{N}_4\text{O}_3$ (*m/e*) 434.416, obsd 435.2 (M + H). ^1H NMR (300 MHz, $\text{DMSO-}d_6$) δ 7.82–7.92 (m, 3H), 7.49–7.67 (m, 3H), 7.40 (dd, J = 2.72, 9.06 Hz, 1H), 6.56 (d, J = 9.06 Hz, 1H), 3.53–3.62 (m, 2H), 3.33–3.37 (m, 2H), 3.31 (s, 3H), 3.08 (s, 3H), 2.90 (s, 3H).

2-Phenyl-5-trifluoromethyloxazole-4-carboxylic Acid {2-[(2-Methoxyethyl)methylamino]pyrimidin-5-yl}amide (9). This compound was prepared by the same method as described for the preparation of compound (**6**) by using 2-chloro-5-nitropyrimidine. LC–MS calcd for $\text{C}_{19}\text{H}_{18}\text{F}_3\text{N}_5\text{O}_3$ (*m/e*) 421.14, obsd 422.0 (M + H). ^1H NMR (300 MHz, CDCl_3) δ 8.57–8.65 (m, 3H), 8.09–8.17 (m, 2H), 7.50–7.65 (m, 3H), 3.80–3.88 (m, 2H), 3.57–3.65 (m, 2H), 3.36 (s, 3H), 3.23 (s, 3H).

2-Phenyl-5-trifluoromethyloxazole-4-carboxylic Acid {4-[(2-Methoxyethyl)methylamino]phenyl}amide (10). This compound was prepared by the same method as described for the preparation of compound (**6**) by using 1-fluoro-4-nitrobenzene. LC–MS calcd for $\text{C}_{21}\text{H}_{20}\text{F}_3\text{N}_3\text{O}_3$ (*m/e*) 419.15, obsd 420.0 (M + H). ^1H NMR (300 MHz, CDCl_3) δ 8.79 (br s, 1H), 8.08–8.20 (m, 2H), 7.49–7.66 (m, 5H), 6.73 (d, J = 8.75 Hz, 2H), 3.46–3.64 (m, 4H), 3.37 (s, 3H), 2.99 (s, 3H).

2-Phenyl-5-trifluoromethyloxazole-4-carboxylic Acid [6-(3-Ethoxyazetidin-1-yl)pyridin-3-yl]amide (11). 2-(3-Ethoxyazetidin-1-yl)-5-nitropyridine (59 mg, 0.264 mmol) was hydrogenated and reacted with 2-phenyl-5-trifluoromethyloxazole-4-carboxylic acid (74 mg, 0.29 mmol), Et_3N (186 μL , 1.32 mmol), and BOP (122 mg, 0.277 mmol). Following workup, the crude material was purified by flash chromatography to yield 2-phenyl-5-trifluoromethyloxazole-4-carboxylic acid [6-(3-ethoxyazetidin-1-yl)pyridin-3-yl]amide as a solid (79 mg, 83%). LC–MS calcd for $\text{C}_{21}\text{H}_{19}\text{F}_3\text{N}_4\text{O}_3$ (*m/e*) 432.41, obsd 433.1 (M + H). ^1H NMR (300 MHz, $\text{DMSO-}d_6$) δ 10.46 (s, 1H), 8.39–8.44 (m, 1H), 8.13 (d, J = 7.55 Hz, 2H), 7.91 (dd, J = 2.26, 8.91 Hz, 1H), 7.56–7.72 (m, 3H), 6.43 (d, J = 9.06 Hz, 1H), 4.34–4.43

(m, 1H), 4.08–4.18 (m, 2H), 3.71 (dd, $J = 4.08, 8.60$ Hz, 2H), 3.43 (q, $J = 6.90$ Hz, 2H), 1.12 (t, $J = 6.90$ Hz, 3H).

(S)-2-Phenyl-5-trifluoromethyloxazole-4-carboxylic Acid-[2-(3-Hydroxypyrrolidin-1-yl)pyrimidin-5-yl]amide (12). To a solution of 2-chloro-5-nitropyrimidine (638 mg, 4 mmol) in THF (15 mL) cooled to 0 °C was added (S)-3-hydroxypyrrolidine (392 mg, 4.5 mmol) and triethylamine (1.2 mL). The mixture was stirred at room temperature overnight. Solids were filtered out, and the solution was concentrated. The residue was extracted with ethyl acetate and water. The organic layer was washed with dilute aqueous citric acid solution. After the evaporation of solvents, the residue was treated with ether/petroleum ether (1:1 ratio) and the white solid was filtered to give *N*-(5-nitropyrimidin-2-yl)pyrrolidin-3-ol (690 mg, 82.1%). LC–MS calcd for $C_8H_{10}N_4O_3$ (m/e) 210.19, obsd 211.0 (ES, M + H). This compound (150 mg, 0.714 mmol) was dissolved in a mixture of THF and methanol, and the solution was hydrogenated at 40 psi in the presence of a catalytic amount of palladium on carbon. The mixture was filtered, and solvents were removed. The residue was treated with 2-phenyl-5-trifluoromethyloxazole-4-carboxylic acid (183.6 mg, 0.714 mmol) and PyBrop (333 mg, 0.714 mmol) in DMF containing triethylamine (0.2 mL). After overnight stirring, the mixture was worked up and the crude mixture was purified through flash column chromatography, eluting with ethyl acetate in hexanes to give a white solid as (S)-2-phenyl-5-trifluoromethyloxazole-4-carboxylic acid [2-(3-hydroxypyrrolidin-1-yl)pyrimidin-5-yl]amide (178 mg, 59.4%). LC–MS calcd for $C_{19}H_{16}F_3N_5O_3$ (m/e) 419.36, obsd 420.1 (ES, M + H). 1H NMR (300 MHz, $CDCl_3$) δ ppm 2.00–2.27 (m, 2H), 3.61–3.87 (m, 4H), 4.56–4.74 (m, 1H), 7.47–7.69 (m, 3H), 8.06–8.20 (m, 2H), 8.66 (s, 3H).

2-Phenyl-5-trifluoromethyloxazole-4-carboxylic Acid [6-(3,3-Difluoroazetidin-1-yl)pyridin-3-yl]amide (13). 3,3-Difluoroazetidine hydrochloride (259 mg, 2 mmol) was mixed with 2-chloro-5-nitropyridine (317 mg, 2 mmol) in THF (8 mL) containing DIPEA (1.4 mL). The mixture was heated in a microwave at 120 °C for 20 min. The resulting mixture was kept at room temperature overnight and then filtered. The solution was evaporated to dryness, and the solid material was triturated with methanol. Filtration of the mixture provided 2-(3,3-difluoroazetidin-1-yl)-5-nitropyridine (288 mg, 67%). 1H NMR (300 MHz, $CDCl_3$) δ ppm 4.53 (t, $J = 11.6$ Hz, 4H), 6.34 (d, $J = 9.1$ Hz, 1H), 8.29 (dd, $J = 9.2, 2.6$ Hz, 1H), 9.07 (s, 1H).

The above material (140 mg, 0.65 mmol) was hydrogenated and then coupled with 2-phenyl-5-trifluoromethyloxazole-4-carboxylic acid (163.9 mg, 0.64 mmol) to provide 2-phenyl-5-trifluoromethyloxazole-4-carboxylic acid [6-(3,3-difluoroazetidin-1-yl)pyridin-3-yl]amide (132.8 mg, 48.1%) as a white crystalline material. LC–MS calcd for $C_{19}H_{13}F_5N_4O_2$ (m/e) 424.32, obsd 425.0 (ES, M + H). 1H NMR (300 MHz, $CDCl_3$) δ ppm 4.39 (t, $J = 12.1$ Hz, 4H), 6.45 (d, $J = 9.1$ Hz, 1H), 7.50–7.67 (m, 3H), 8.15 (d, $J = 7.5$ Hz, 2H), 8.24 (dd, $J = 8.6, 2.6$ Hz, 1H), 8.31 (s, 1H), 8.82 (br s, 1H).

(1-{5-[(2-Phenyl-5-trifluoromethyloxazole-4-carbonyl)amino]pyridin-2-yl}azetidin-3-yloxy)acetic Acid Hydrochloride (14). 2-Bromo-5-nitropyridine (1.82 g, 8.96 mmol), azetidin-3-ol hydrochloride (0.98 g, 9.0 mol), and potassium carbonate (3.71 g, 26.8 mmol) in 40 mL of NMP were stirred at 80 °C for 24 h under argon. After cooling, the reaction mixture was diluted with 150 mL of EtOAc, washed with 4 × 25 mL of brine, dried over magnesium sulfate, filtered, and evaporated to furnish an oil. The crude material was then dissolved in 100 mL of ethyl acetate and eluted through a plug of silica gel and evaporated to yield 1-(5-nitropyridin-2-yl)azetidin-3-ol as a yellow solid (1.0 g, 57%). LC–MS calcd for $C_8H_9N_3O_3$ (m/e) 195.18, obsd 196.0 (ES, M + H).

A mixture of 1-(5-nitropyridin-2-yl)azetidin-3-ol (176 mg, 0.9 mmol) and sodium hydride (60% in oil, 108 mg, 2.7 mmol) in 3 mL of THF and 3 mL of DMF was stirred in an ice bath under argon for 40 min. *tert*-Butyl bromoacetate (199.7 μ L, 1.35 mmol) was added, and the resulting mixture

was stirred at room temperature for 2 h. The reaction mixture was diluted with 100 mL of ethyl acetate and extracted with 3 × 25 mL of saturated sodium bicarbonate solution, 25 mL of brine, dried over magnesium sulfate, filtered, and evaporated to give a dark oil. The crude material was applied to a short silica plug and eluted with hexanes and ether. The ether fraction was evaporated to yield [1-(5-nitropyridin-2-yl)azetidin-3-yloxy]acetic acid *tert*-butyl ester as a bright yellow solid (210 mg, 76%). LC–MS calcd for $C_{14}H_{19}N_3O_5$ (m/e) 309.32, obsd 310.1 (ES, M + H).

[1-(5-Nitropyridin-2-yl)azetidin-3-yloxy]acetic acid *tert*-butyl ester (210 mg, 0.679 mmol) was hydrogenated at 40 psi in methanol. The mixture was filtered, and solvents were evaporated. The residue was treated with 2-phenyl-5-trifluoromethyloxazole-4-carboxylic acid (183 mg, 0.71 mmol), DIPEA (355 μ L, 2.03 mmol), and BOP (315 mg, 0.74 mmol) in 3 mL of DMF. After overnight stirring, solvents were evaporated and the residue was extracted with ethyl acetate and water. The crude product was purified through flash column chromatography, eluting with ethyl acetate in hexanes to give 1-{5-[(2-phenyl-5-trifluoromethyloxazole-4-carbonyl)amino]pyridin-2-yl}azetidin-3-yloxy)acetic acid *tert*-butyl ester as a light brown solid (169 mg, 48%). LC–MS calcd for $C_{25}H_{25}F_3N_4O_5$ (m/e) 518.5, obsd 519.1 (M + H).

1-{5-[(2-Phenyl-5-trifluoromethyloxazole-4-carbonyl)amino]pyridin-2-yl}azetidin-3-yloxy)acetic acid *tert*-butyl ester (132 mg, 0.26 mmol) was treated with 8 mL of 97% TFA in water at room temperature for 1 h. The reaction mixture was evaporated, re-evaporated from 1 N HCl in CH_3CN , and dried under vacuum to yield 1-{5-[(2-phenyl-5-trifluoromethyloxazole-4-carbonyl)amino]pyridin-2-yl}azetidin-3-yloxy)acetic acid hydrochloride as an off-white solid (130 mg, 100%). LC–MS calcd for $C_{21}H_{17}F_3N_4O_5$ (m/e) 462.39, obsd 463.0 (M + H). 1H NMR (300 MHz, $DMSO-d_6$) δ 10.81 (s, 1H), 8.48 (d, $J = 2.11$ Hz, 1H), 8.22 (d, $J = 9.2$ Hz, 1H), 8.13 (d, $J = 6.34$ Hz, 2H), 7.58–7.74 (m, 3H), 6.87 (d, $J = 9.2$ Hz, 1H), 4.56 (m, 1H), 4.33–4.46 (m, 2H), 4.13 (s, 2H), 4.04–4.11 (m, 2H).

2-Phenyl-5-trifluoromethyloxazole-4-carboxylic Acid (6-Piperazin-1-ylpyridin-3-yl)amide Hydrochloride (31). 4-(5-Aminopyridin-2-yl)piperazine-1-carboxylic acid *tert*-butyl ester (834 mg, 3.0 mmol) was mixed with 2-phenyl-5-trifluoromethyloxazole-4-carboxylic acid (771 mg, 3.0 mmol) and bromotrispyrrolidinophosphonium hexafluorophosphate (1.398 g, 3 mmol) in *N,N*-dimethylformamide (20 mL) and methylene chloride (5 mL) containing triethylamine (0.85 mL). The mixture was stirred at room temperature overnight, and the solvents were evaporated. The residue was partitioned between ethyl acetate and water. The organic layer was dried over sodium sulfate, and solvent was evaporated. The residue was triturated with ethyl acetate and the solid was filtered to give 4-{5-[(2-phenyl-5-trifluoromethyloxazole-4-carbonyl)amino]pyridin-2-yl}piperazine-1-carboxylic acid *tert*-butyl ester (1.09 g, 70.3%). LC–MS calcd for $C_{25}H_{26}F_3N_5O_4$ (m/e) 517.5, obsd 518.1 (M + H). 1H NMR (300 MHz, $DMSO-d_6$) δ ppm 1.42 (s, 9H), 3.44 (d, $J = 4.2$ Hz, 8H), 6.90 (d, $J = 9.4$ Hz, 1H), 7.56–7.74 (m, 3H), 7.98 (dd, $J = 9.2, 2.6$ Hz, 1H), 8.15 (dd, $J = 8.0, 1.7$ Hz, 2H), 8.51 (d, $J = 2.7$ Hz, 1H), 10.52 (s, 1H).

4-{5-[(2-Phenyl-5-trifluoromethyloxazole-4-carbonyl)amino]pyridin-2-yl}piperazine-1-carboxylic acid *tert*-butyl ester (300 mg, 0.58 mmol) prepared above was suspended in methylene chloride (5 mL) and methanol (5 mL). To this mixture was added hydrogen chloride in ether (4 N, 3 mL). The mixture was stirred at room temperature overnight. Solvents were evaporated, and the residue was dried in vacuum. The resulting solid was triturated with dry ether and then filtered to give a hydrochloride salt of 2-phenyl-5-trifluoromethyloxazole-4-carboxylic acid (6-piperazin-1-ylpyridin-3-yl)amide (274 mg, 96.5%). LC–MS calcd for the free base $C_{20}H_{18}F_3N_5O_2$ (m/e) 417.39, obsd 418.0 (M + H). 1H NMR (300 MHz, methanol- d_4) δ ppm 3.49 (d, $J = 4.8$ Hz, 4H), 4.00 (br s, 4H), 7.53 (d, $J = 10.0$ Hz, 1H), 7.57–7.70 (m, 3H), 8.20 (d, $J = 6.6$ Hz, 2H), 8.42 (d, $J = 10.0$ Hz, 1H), 8.85 (s, 1H).

2-Phenyl-5-trifluoromethyloxazole-4-carboxylic Acid (2-Piperazin-1-ylpyrimidin-5-yl)amide Hydrochloride (32). This compound was prepared according to the same method as described for the preparation of compound 31. LC–MS calcd for the free base $C_{19}H_{17}F_3N_6O_2$ (m/e) 418.14, obsd 419.0 ($M + H$). 1H NMR (300 MHz, $DMSO-d_6$) δ ppm 3.16 (br s, 4 H), 3.78–4.09 (m, 4 H), 7.46–7.85 (m, 3 H), 8.14 (dd, $J = 7.8, 1.5$ Hz, 2 H), 8.80 (s, 2 H), 9.39 (br s, 2 H, NH, HCl), 10.71 (s, 1 H, amide).

2-Phenyl-5-trifluoromethyloxazole-4-carboxylic Acid (4-Piperazin-1-ylphenyl)amide (33). This compound was prepared according to the same method as described for the preparation of compound 31. LC–MS calcd for $C_{21}H_{19}F_3N_4O_2$ (m/e) 416.14, obsd 417.1 ($M + H$). 1H NMR (300 MHz, $CDCl_3$) δ ppm 3.05–3.10 (m, 4 H), 3.11–3.25 (m, 4 H), 6.90–6.98 (m, 2 H), 7.42–7.77 (m, 5 H), 8.14 (dd, $J = 7.8, 1.5$ Hz, 2 H), 8.84 (s, 1 H).

2-Phenyl-5-trifluoromethyloxazole-4-carboxylic Acid (4-Piperidin-4-ylphenyl)amide (34). This compound was prepared from 2-phenyl-5-trifluoromethyloxazole-4-carboxylic acid and 4-(4-aminophenyl)piperidine-1-carboxylic acid *tert*-butyl ester. 4-{4-[(2-Phenyl-5-trifluoromethyloxazole-4-carbonyl)amino]phenyl}piperidine-1-carboxylic acid *tert*-butyl ester (245 mg, 0.475 mmol) was dissolved in methylene chloride (2 mL) and trifluoroacetic acid (1 mL). The mixture was stirred at room temperature, and the solvents were evaporated. The residue was extracted with dichloromethane and diluted sodium hydroxide solution. The organic layer was washed with brine and dried over sodium sulfate. Evaporation of solvents gave 2-phenyl-5-trifluoromethyloxazole-4-carboxylic acid (4-piperidin-4-yl-phenyl)amide (183 mg, 92.8%) as a white solid. LC–MS calcd for $C_{22}H_{20}F_3N_3O_2$ (m/e) 415.15, obsd 416.0. 1H NMR (300 MHz, $CDCl_3$) δ ppm 1.55–1.76 (m, 3 H), 1.85 (d, $J = 12.4$ Hz, 2 H), 2.64 (t, $J = 12.1$ Hz, 1 H), 2.76 (t, $J = 11.8$ Hz, 2 H), 3.21 (d, $J = 11.2$ Hz, 2 H), 7.24 (br s, 2 H), 7.49–7.62 (m, 3 H), 7.68 (d, $J = 8.5$ Hz, 2H), 8.15 (d, $J = 6.6$ Hz, 2H), 8.90 (br s, 1H).

2-Phenyl-5-trifluoromethyloxazole-4-carboxylic Acid (1',2',3',4',5',6'-Hexahydro[2,4']bipyridinyl-5-yl)amide (35). To a mixture of 2-bromo-5-nitropyridine (0.5 g, 2.46 mmol) and *N*-*tert*-butoxycarbonyl-1,2,3,6-tetrahydropyridine-4-boronic acid pinacol ester (0.913 g, 2.95 mmol) in toluene (4 mL) and ethanol (1.0 mL) were added potassium carbonate solution (2M, 2 mL) and $PdCl_2dppf$ (180 mg, 0.246 mmol). The mixture was degassed with argon and heated at 100 °C in a microwave for 40 min with stirring. Solvents were evaporated, and the residue was extracted with ethyl acetate. After evaporation of the solvents, the residue was purified using flash chromatography (eluting with ethyl acetate and hexanes) to give 5-nitro-3',6'-dihydro-2'*H*-[2,4']bipyridinyl-1'-carboxylic acid *tert*-butyl ester as a solid (400 mg, 53.2%). This solid material (400 mg) was dissolved in methanol (50 mL) and tetrahydrofuran (10 mL). To this mixture was added 10% palladium on carbon (100 mg). The mixture was hydrogenated at 50 psi for 2 h. The mixture was filtered and the solvents were evaporated to give 5-amino-3',4',5',6'-tetrahydro-2'*H*-[2,4']bipyridinyl-1'-carboxylic acid *tert*-butyl ester as a white solid (363 mg, 100%). This amine (363 mg) was coupled with 2-phenyl-5-trifluoromethyloxazole-4-carboxylic acid to provide 5-[(2-phenyl-5-trifluoromethyloxazole-4-carbonyl)amino]-3',4',5',6'-tetrahydro-2'*H*-[2,4']bipyridinyl-1'-carboxylic acid *tert*-butyl ester (535 mg, 79.1%). This amide (535 mg) was dissolved in a mixture of methylene chloride (35 mL) and trifluoroacetic acid (9 mL). The mixture was stirred at room temperature for 2 h. Solvents were evaporated, and the residues were partitioned between methylene chloride and diluted sodium hydroxide solution. The organic layer was washed with brine and dried over sodium sulfate. Evaporation of solvents gave 2-phenyl-5-trifluoromethyloxazole-4-carboxylic acid (1',2',3',4',5',6'-hexahydro[2,4']bipyridinyl-5-yl)-amide (360 mg, 83.5%) as a solid. LC–MS calcd for $C_{21}H_{19}F_3N_4O_2$ (m/e) 416.15, obsd 417.1 ($M + H$). 1H NMR (300 MHz, CD_3OD) δ ppm 1.64–1.82 (m, 2 H), 1.85–2.00 (m, 2 H), 2.67–2.96 (m, 3 H), 3.18

(d, $J = 12.4$ Hz, 2 H), 7.37 (d, $J = 8.5$ Hz, 1 H), 7.54–7.69 (m, 3 H), 8.11–8.30 (m, 3 H), 8.86 (d, $J = 2.4$ Hz, 1 H).

2-Phenyl-5-trifluoromethyloxazole-4-carboxylic Acid [6-(4-Cyclopropanecarbonylpiperazin-1-yl)pyridin-3-yl]-amide (15). Compound 31 (40 mg) was suspended in dichloromethane (4 mL) containing triethylamine (0.07 mL) and cyclopropyl-carbonyl chloride (0.01 mL) while the reaction mixture was cooled with an ice bath. The mixture was stirred at room temperature overnight, and solvents were evaporated. The residue was extracted with dichloromethane and brine. After evaporation of solvents, the residue was triturated with methanol. The white solid was filtered to give 2-phenyl-5-trifluoromethyloxazole-4-carboxylic acid [6-(4-cyclopropanecarbonylpiperazin-1-yl)pyridin-3-yl]amide (30 mg, 76%). LC–MS calcd for $C_{24}H_{22}F_3N_5O_3$ (m/e) 485.17, obsd 486.1 ($M + H$). 1H NMR (300 MHz, $CDCl_3$) δ ppm 0.82 (dq, $J = 7.2, 3.6$ Hz, 2 H), 0.95–1.09 (m, 2 H), 1.69–1.87 (m, 1 H), 3.51 (d, $J = 7.2$ Hz, 2 H), 3.68 (br s, 2 H), 3.81 (br s, 4 H), 6.71 (d, $J = 9.4$ Hz, 1 H), 7.49–7.67 (m, 3 H), 8.08–8.27 (m, 3 H), 8.34 (d, $J = 2.4$ Hz, 1 H), 8.81 (s, 1 H).

4-{5-[(2-Phenyl-5-trifluoromethyloxazole-4-carbonyl)-amino]pyridin-2-yl}piperazine-1-carboxylic Acid Methyl Ester (16). Compound 16 was prepared from compound 31 and methyl chloroformate using the same method as described for the preparation of compound 15 (75%). LC–MS calcd for $C_{22}H_{20}F_3N_5O_4$ (m/e) 475.15, obsd 476.1 ($M + H$). 1H NMR (300 MHz, $CDCl_3$) δ ppm 3.56 (d, $J = 5.7$ Hz, 4 H), 3.61 (br s, 4 H), 3.75 (s, 3 H), 6.71 (d, $J = 9.1$ Hz, 1 H), 7.50–7.66 (m, 3 H), 8.08–8.24 (m, 3 H), 8.32 (d, $J = 2.4$ Hz, 1 H), 8.81 (s, 1 H).

4-{5-[(2-Phenyl-5-trifluoromethyloxazole-4-carbonyl)-amino]pyridin-2-yl}piperazine-1-carboxylic Acid Ethyl Ester (17). Compound 17 was prepared from compound 31 and ethyl chloroformate using the same method as described for the preparation of compound 15 (77%). LC–MS calcd for $C_{23}H_{22}F_3N_5O_4$ (m/e) 489.16, obsd 490.0 ($M + H$). 1H NMR (300 MHz, $CDCl_3$) δ ppm 1.30 (t, $J = 7.1$ Hz, 3 H), 3.59 (d, $J = 11.5$ Hz, 8 H), 4.19 (q, $J = 6.9$ Hz, 2 H), 6.71 (d, $J = 9.1$ Hz, 1 H), 7.51–7.66 (m, 3 H), 8.15 (d, $J = 8.2$ Hz, 2 H), 8.21 (d, $J = 8.8$ Hz, 1 H), 8.32 (d, $J = 2.4$ Hz, 1 H), 8.81 (s, 1 H).

4-{5-[(2-Phenyl-5-trifluoromethyloxazole-4-carbonyl)amino]-pyrimidin-2-yl}piperazine-1-carboxylic Acid Methyl Ester (18). Compound 18 was prepared from compound 32 and methyl chloroformate (80.4%). LC–MS calcd for $C_{21}H_{19}F_3N_6O_4$ (m/e) 476.14, obsd 477.0 ($M + H$). 1H NMR (300 MHz, $CDCl_3$) δ ppm 3.52–3.63 (m, 4 H), 3.76 (s, 3 H), 3.80–3.93 (m, 4 H), 7.49–7.68 (m, 3 H), 8.14 (dd, $J = 8.0, 1.4$ Hz, 2 H), 8.59–8.78 (m, 3 H).

2-Phenyl-5-trifluoromethyloxazole-4-carboxylic Acid (1'-Cyclopropanecarbonyl-1',2',3',4',5',6'-hexahydro[2,4']bipyridinyl-5-yl)amide (19). To a mixture of compound 35 (50 mg, 0.12 mmol) and cyclopropane carboxylic acid (31 mg, 0.37 mmol) in dichloromethane (5 mL) were added triethylamine (0.06 mL, 0.41 mmol) and BOP reagent (55.7 mg, 0.13 mmol). The mixture was stirred at room temperature for 3 h, and solvents were evaporated. The residue was extracted with ethyl acetate and dried. Solvents were evaporated and the residue was triturated with ether and petroleum ether (1:1 ratio) to give an off white solid as compound 19 (77.6%). LC–MS calcd for $C_{25}H_{23}F_3N_4O_3$ (m/e) 484.17, obsd 485.1 ($M + H$). 1H NMR (300 MHz, $CDCl_3$) δ ppm 0.77 (dd, $J = 7.8, 3.0$ Hz, 2 H), 1.01 (br s, 2 H), 1.80 (td, $J = 8.1, 4.4$ Hz, 3 H), 1.93–2.15 (m, 2 H), 2.73 (t, $J = 11.0$ Hz, 1 H), 3.01 (t, $J = 11.8$ Hz, 1 H), 3.25 (t, $J = 12.2$ Hz, 1 H), 4.39 (d, $J = 13.0$ Hz, 1 H), 4.79 (d, $J = 10.6$ Hz, 1 H), 7.23 (d, $J = 8.5$ Hz, 1 H), 7.51–7.68 (m, 3 H), 8.16 (d, $J = 7.8$ Hz, 2 H), 8.39 (dd, $J = 8.5, 2.4$ Hz, 1 H), 8.65 (d, $J = 2.4$ Hz, 1 H), 8.98 (s, 1 H).

5-[(2-Phenyl-5-trifluoromethyloxazole-4-carbonyl)amino]-3',4',5',6'-tetrahydro-2'*H*-[2,4']bipyridinyl-1'-carboxylic Acid Methyl Ester (20). Compound 20 was prepared from compound 35 and methyl chloroformate (65%). LC–MS calcd for $C_{23}H_{21}F_3N_4O_4$

(*m/e*) 474.15, obsd 475.1 (M + H). ¹H NMR (300 MHz, CDCl₃) δ ppm 1.63–1.83 (m, 2 H), 1.97 (d, *J* = 12.7 Hz, 2 H), 2.93 (m, 3 H), 3.72 (s, 3 H), 4.30 (br s, 2 H), 7.22 (d, *J* = 6.9 Hz, 1 H), 7.49–7.69 (m, 3 H), 8.16 (d, *J* = 7.2 Hz, 2 H), 8.43 (d, *J* = 6.9 Hz, 1 H), 8.68 (br s, 1 H), 9.03 (br s, 1 H).

2-Phenyl-5-trifluoromethyloxazole-4-carboxylic Acid [4-(4-Cyclopropanecarbonylpiperazin-1-yl)phenyl]amide (21). Compound 21 was prepared from compound 33 and cyclopropane carboxylic acid. LC–MS calcd for C₂₅H₂₃F₃N₄O₃ (*m/e*) 484.17, obsd 485.2 (M + H). ¹H NMR (300 MHz, CDCl₃) δ ppm 0.81 (d, *J* = 4.5 Hz, 2 H), 1.03 (br s, 2 H), 1.79 (br s, 1 H), 3.21 (d, *J* = 14.5 Hz, 4 H), 3.85 (br s, 4 H), 6.97 (d, *J* = 8.2 Hz, 2 H), 7.48–7.62 (m, 3 H), 7.68 (d, *J* = 7.8 Hz, 2 H), 8.14 (d, *J* = 7.2 Hz, 2 H), 8.86 (br s, 1 H).

4-{4-[(2-Phenyl-5-trifluoromethyloxazole-4-carbonyl)-amino]phenyl}piperazine-1-carboxylic Acid Methyl Ester (22). Compound 22 was prepared from compound 33 and methyl chloroformate. LC–MS calcd for C₂₃H₂₁F₃N₄O₄ (*m/e*) 474.15, obsd 475.2 (M + H). ¹H NMR (300 MHz, CDCl₃) δ ppm 3.15 (br s, 4 H), 3.65 (br s, 4 H), 3.75 (s, 3 H), 6.96 (d, *J* = 8.2 Hz, 2 H), 7.49–7.62 (m, 3 H), 7.66 (d, *J* = 8.5 Hz, 2 H), 8.14 (d, *J* = 6.9 Hz, 2 H), 8.86 (br s, 1 H).

4-{4-[(2-Phenyl-5-trifluoromethyloxazole-4-carbonyl)-amino]phenyl}piperidine-1-carboxylic Acid Methyl Ester (24). Compound 24 was prepared from compound 34 and methyl chloroformate (80.6%). LC–MS calcd for C₂₄H₂₂F₃N₃O₄ (*m/e*) 473.16, obsd 474.1 (M + H). ¹H NMR (300 MHz, CDCl₃) δ ppm 1.64 (qd, *J* = 12.6, 4.4 Hz, 2 H), 1.86 (d, *J* = 12.1 Hz, 2 H), 2.61–2.74 (m, 1 H), 2.88 (t, *J* = 11.9 Hz, 2 H), 3.73 (s, 3 H), 4.30 (d, *J* = 12.1 Hz, 2 H), 7.23 (d, *J* = 8.5 Hz, 2 H), 7.52–7.62 (m, 3 H), 7.69 (d, *J* = 8.5 Hz, 2 H), 8.15 (dd, *J* = 8.2, 1.5 Hz, 2 H), 8.91 (s, 1 H).

trans-Cyclohexane-1,4-dicarboxylic Acid Monobenzyl Ester (36). To a suspension of *trans*-cyclohexane-1,4-dicarboxylic acid (5 g, 29 mmol) in THF (60 mL) was added oxalyl chloride (2 N in dichloromethane, 15 mL) and two drops of DMF. The mixture was stirred at room temperature for 3 h. The mixture was evaporated to dryness, and the residue was treated with benzyl alcohol (5 mL). The mixture was heated at 80 °C for 20 min and then crystallized from hexanes to give white needle crystals as *trans*-cyclohexane-1,4-dicarboxylic acid monobenzyl ester (3.2 g, 41%). LC–MS calcd for C₁₅H₁₈O₄ (*m/e*) 262.12, obsd 261.0 (M – H). ¹H NMR (300 MHz, DMSO-*d*₆) δ ppm 1.22–1.47 (m, 4 H), 1.80–2.03 (m, 4 H), 2.10–2.24 (m, 1 H), 2.27–2.43 (m, 1 H), 5.08 (s, 2 H), 7.23–7.46 (m, 5 H), 12.09 (s, 1 H).

4-(4-{5-[(2-Phenyl-5-trifluoromethyloxazole-4-carbonyl)-amino]pyridin-2-yl}piperazine-1-carbonyl)-*trans*-cyclohexanecarboxylic Acid (25). This compound was prepared from the amide coupling of 2-phenyl-5-trifluoromethyloxazole-4-carboxylic acid (6-piperazin-1-ylpyridin-3-yl)amide hydrochloride (compound 31) and *trans*-1,4-cyclohexane dicarboxylic acid using coupling reagent BOP in DMF (25%). LC–MS calcd for C₂₈H₂₈F₃N₅O₅ (*m/e*) 571.20, obsd 572.2 (M + H). ¹H NMR (300 MHz, DMSO-*d*₆) δ ppm 1.40 (t, *J* = 10.4 Hz, 4 H), 1.72 (d, *J* = 6.9 Hz, 2 H), 1.84–1.99 (m, 2 H), 2.17 (br s, 1 H), 2.63 (br s, 1 H), 3.40–3.60 (m, 8 H), 6.90 (d, *J* = 9.1 Hz, 1 H), 7.57–7.73 (m, 3 H), 7.98 (dd, *J* = 9.2, 2.6 Hz, 1 H), 8.09–8.21 (m, 2 H), 8.51 (d, *J* = 2.4 Hz, 1 H), 10.52 (s, 1 H), 12.05 (s, 1 H).

4-{5-[(2-Phenyl-5-trifluoromethyloxazole-4-carbonyl)amino]-3',4',5',6'-tetrahydro-2'*H*-[2,4']bipyridinyl-1'-carbonyl}-*trans*-cyclohexanecarboxylic Acid (26). This compound was prepared from the amide coupling of 2-phenyl-5-trifluoromethyloxazole-4-carboxylic acid (1',2',3',4',5',6'-hexahydro[2,4']bipyridinyl-5-yl)amide (compound 35) and *trans*-1,4-cyclohexane dicarboxylic acid using coupling reagent BOP in DMF (31%). LC–MS calcd for C₂₉H₂₉F₃N₄O₅ (*m/e*) 570.21, obsd 571.2 (M + H). ¹H NMR (300 MHz, CDCl₃) δ ppm 1.39–1.79 (m, 5 H), 1.81–2.07 (m, 5 H), 2.16 (br s, 2 H), 2.39 (d, *J* = 11.8 Hz, 1 H), 2.49–2.78 (m, 2 H), 2.99 (br s, 1 H),

3.18 (t, *J* = 12.2 Hz, 1 H), 4.07 (d, *J* = 12.1 Hz, 1 H), 4.83 (d, *J* = 10.6 Hz, 1 H), 7.23 (d, *J* = 8.2 Hz, 1 H), 7.50–7.70 (m, 3 H), 8.17 (d, *J* = 7.2 Hz, 2 H), 8.52 (d, *J* = 8.2 Hz, 1 H), 8.72 (br s, 1 H), 9.04 (s, 1 H).

4-(4-{4-[(2-Phenyl-5-trifluoromethyloxazole-4-carbonyl)-amino]phenyl}piperazine-1-carbonyl)-*trans*-cyclohexanecarboxylic Acid (27). This compound was prepared from the amide coupling of 2-phenyl-5-trifluoromethyloxazole-4-carboxylic acid (4-piperazin-1-yl-phenyl)amide (compound 33) and *trans*-1,4-cyclohexane dicarboxylic acid using coupling reagent BOP in DMF (37 mg, 32%). LC–MS calcd for C₂₉H₂₉F₃N₄O₅ (*m/e*) 570.21, obsd 571.0 (M + H). ¹H NMR (300 MHz, DMSO-*d*₆) δ 10.38 (s, 1H), 8.13 (d, *J* = 6.64 Hz, 2H), 7.55–7.72 (m, 5H), 6.97 (d, *J* = 8.75 Hz, 2H), 3.60 (br d, *J* = 13.30 Hz, 4H), 3.08 (br d, *J* = 15.40 Hz, 4H), 2.52–2.59 (m, 1H), 1.83–1.94 (m, 2H), 1.63–1.78 (m, 2H), 1.31–1.45 (m, 4H).

4-(4-{4-[(2-Phenyl-5-trifluoromethyloxazole-4-carbonyl)-amino]phenyl}piperazine-1-carbonyl)-*cis*-cyclohexanecarboxylic Acid (28). This compound was prepared from the amide coupling of 2-phenyl-5-trifluoromethyloxazole-4-carboxylic acid (4-piperazin-1-yl-phenyl)amide (compound 33) and *cis*-1,4-cyclohexane dicarboxylic acid using coupling reagent BOP in DMF (15 mg, 9%). LC–MS calcd for C₂₉H₂₉F₃N₄O₅ (*m/e*) 570.21, obsd 571.2 (M + H). ¹H NMR (300 MHz, DMSO-*d*₆) δ 12.12 (br s, 1H), 10.39 (s, 1H), 8.13 (br d, *J* = 9.0 Hz, 2H), 7.54–7.75 (m, 5H), 6.96 (d, *J* = 9.0 Hz, 2H), 3.48–3.70 (m, 4H), 2.97–3.19 (m, 4H), 2.60–2.77 (m, 1H), 1.88–2.07 (m, 2H), 1.41–1.63 (m, 6H).

4-(4-{4-[(2-Phenyl-5-trifluoromethyloxazole-4-carbonyl)-amino]phenyl}piperidine-1-carbonyl)-*trans*-cyclohexanecarboxylic Acid (29). To a solution of compound 36 (2.62 g, 10.0 mmol) in dichloromethane (60 mL) was added oxalyl chloride (10 mL, 2 N in dichloromethane) and one drop of DMF. The resulting solution was stirred at room temperature for 1 h until gas evolution ceased. Solvents were evaporated, and the residue was treated with benzene (20 mL). Solvents were evaporated, and the waxy material was dried under vacuum. This material was dissolved in dichloromethane (30 mL), and the solution was added dropwise to a dichloromethane solution (100 mL) containing compound 34 (4.15 g, 10 mmol) and triethylamine (2.8 mL) under ice bath. The solution was stirred for 30 min, and the ice bath was removed. After 3 h of stirring at room temperature, the solution was extracted with dichloromethane and 0.2 N hydrochloric acid. The organic layer was washed with water and sodium bicarbonate solution, dried over sodium sulfate, and concentrated. The residue was passed through silica gel plug eluted with ethyl acetate in hexanes. After evaporation of solvents, a pale yellow fluffy material was obtained (6.46 g, 98%). This material was dissolved in a solution containing THF (10 mL) and ethanol (100 mL) in the presence of palladium on carbon (10%, 0.95 g). The mixture was hydrogenated at 45 psi on a Parr shaker until TLC indicated complete consumption of the starting material. The mixture was filtered through a layer of Celite and concentrated. The residue was crystallized from ethyl acetate to provide compound 29 as a white solid (4.55 g, 80%). Mp 208–209 °C. HRMS calcd for C₃₀H₃₀F₃N₃O₅ (M + H) 570.2211, obsd 570.2210. ¹H NMR (300 MHz, DMSO-*d*₆) δ ppm 1.32–1.61 (m, 6 H), 1.64–1.98 (m, 6 H), 2.17 (br s, 1 H), 2.59 (d, *J* = 11.8 Hz, 2 H), 2.76 (t, *J* = 11.5 Hz, 1 H), 3.10 (t, *J* = 12.4 Hz, 1 H), 4.08 (d, *J* = 13.9 Hz, 1 H), 4.56 (d, *J* = 12.1 Hz, 1 H), 7.26 (d, *J* = 8.8 Hz, 2 H), 7.58–7.77 (m, 5 H), 8.15 (dd, *J* = 7.8, 1.5 Hz, 2 H), 10.53 (s, 1 H), 12.04 (br s, 1 H). Elemental analysis calcd, C 63.26%, H 5.31%, N 7.38%; obsd, C 63.19%, H 5.34%, N 7.31%.

4-(4-{4-[(2-Phenyl-5-trifluoromethyloxazole-4-carbonyl)-amino]phenyl}piperidine-1-carbonyl)-*cis*-cyclohexanecarboxylic Acid (30). This compound was prepared from the amide coupling of 2-phenyl-5-trifluoromethyloxazole-4-carboxylic acid (4-piperidin-4-yl-phenyl)amide (compound 34) and *cis*-1,4-cyclohexane dicarboxylic acid using coupling reagent BOP in DMF. HRMS calcd for C₃₀H₃₀F₃N₃O₅ (M + H) 570.2211, obsd 570.2210. ¹H NMR (300 MHz,

DMSO- d_6 δ ppm 12.13 (br s, 1 H), 10.53 (s, 1 H), 8.15 (dd, $J = 7.8, 1.5$ Hz, 2 H), 7.58–7.78 (m, 5 H), 7.26 (d, $J = 8.5$ Hz, 2 H), 4.55 (d, $J = 12.1$ Hz, 1 H), 4.05 (d, $J = 14.2$ Hz, 1 H), 3.10 (t, $J = 12.4$ Hz, 1 H), 2.61–2.84 (m, 2 H), 2.44–2.58 (m, 2 H), 2.00 (d, $J = 7.8$ Hz, 2 H), 1.70–1.88 (m, 2 H), 1.22–1.65 (m, 8 H).

PatchXpress hERG Inhibition Assay. The detailed method to quantify hERG channel inhibition by the automated patch clamp system PatchXpress 7000A (Molecular Devices, Sunnyvale, CA) has been described elsewhere.²⁵ In brief, Chinese hamster ovary (CHO) cells transfected with the human ether-a-go-go-related gene (hERG) was cultured in Ex-cell 302 medium supplemented with 10% fetal bovine serum, 2 mM glutamine, and 0.25 mg/mL Geneticin and maintained in a CO₂ incubator at 37 °C. For patch clamp electrophysiology, the external buffer contained the following (in mM): 150 NaCl, 10 Hepes, 4 KCl, 1.2 CaCl₂, 1 MgCl₂. pH 7.4 was adjusted with HCl. The internal recording solution contained the following (in mM): 140 KCl, 6 EGTA, 5 Hepes, MgCl₂, 5 ATP-Na₂. pH 7.2 was adjusted with KOH. Once the cell was loaded in the recording chamber and formed a gigaohm seal with the planar glass electrodes (Sealchip), a whole-cell configuration was achieved by rupturing the cell membrane. The membrane potential was then clamped at –80 mV and the hERG channel activated by a 1 s depolarizing pulse delivered at 0.1 Hz. The hERG current was measured during the 500 ms repolarizing pulse to –40 mV. After an acceptable hERG current recording was obtained, the cell was first exposed to 0.3% DMSO as the vehicle control followed by the test article in three ascending, full log interval concentrations and finally E-4031 at 1 μ M (as the positive control) to block the hERG current completely. Each test article was tested on three or more cells and at concentrations up to 30 μ M or the solubility limit, determined using the BD Gentest solubility scanner (BD Biosciences, San Jose, CA). The inhibition of hERG current at each concentration was normalized to that recorded in the vehicle control and fitted with Hill equation to calculate IC₂₀ and/or IC₅₀.

Pharmacokinetic Analysis. Hanover Wistar rats ($n = 3$) were cannulated in jugular and femoral vein. Rats were dosed either intravenously via jugular vein or by oral gavage, and blood samples were collected via femoral vein. Plasma was separated after centrifugation and transferred into tubes containing EDTA. Beagle dogs ($n = 3$) were dosed intravenously or via oral gavage. Compounds were formulated as the following: iv 5 mg/kg solution in 2% DMA, 15% PEG400, 77% of 28% HP β CD in 0.25 M, pH 7 phosphate buffered saline, po 2 mg/mL suspension in 2% Klucel LF, and 0.1% Tween 80 in water. Quantitative analysis of DGAT inhibitors in rat and dog plasma was carried out as follows: Plasma levels of DGAT inhibitors were determined using LC/MS/MS. Briefly, the compounds were extracted from plasma by protein precipitation with acetonitrile. The extracts were diluted with an equal volume of water and injected to a C18 column and analyzed by LC–MS/MS to quantitate the compounds. The linear range of the method was 5.0–5000 ng/mL. PK analysis was performed using a noncompartmental model.

DGAT Inhibition Cell Assay. Media, FBS, and supplements were all from GIBCO (DMEM/F12 (Gibco no. 11330-032) + 10% FBS + 1% L-glutamine + 20 μ L G418/mL medium, DMEM high glucose). The fatty acid free BSA, fraction V, was from Roche. TLC plates (20 cm \times 20 cm silica gel 60 F 254, no. 5735/7 EM Science) were ordered from VWR. ¹⁴C palmitic acid (no. NEC 075H, 0.25 mCi/2.5 mL, 55.0 mCi/mmol) was obtained from PerkinElmer Life Sciences.

A CHO cell line that expresses DGAT1 (CHOK1/DGAT) was plated at a density of 2.5×10^5 cells/well in six-well plates in DMEM/F12 medium. The next day, medium was removed and the cells were washed twice with phosphate buffered saline (PBS). PBS was removed, and DMEM high glucose with 0.01% BSA (fatty acid free) was added together with tested compounds at multiple dilutions starting at 25 μ M. Then 0.5 μ Ci ¹⁴C palmitic acid was added to each well. The cells were incubated for 1 h at 37 °C with the reaction terminated by placing the

plate on ice, scraping cells into medium, and then combining with chloroform/methanol to extract lipids. Extracted lipids were resolved on TLC plates in solvent containing petroleum ether, ether, acetic acid (80:20:1, v:v:v). The resolved lipids were identified and quantified by phosphoimager analysis.

Inhibition on Body Weight Gain. Male DIO rats, 19 weeks old, on HFD for 12 weeks were treated with compound 29 at 0.3, 1, and 3 mg/kg, po, in Klucel (hydroxypropyl cellulose) suspension for 22 days. Body weight and food intake were measured for the duration of the experiment. On day 21, an OGTT was performed, and on day 22 animals were euthanized and organ weights and fat pads were measured. Plasma was collected, and lipids were analyzed.

Oral Glucose Tolerance Test. Male Sprague–Dawley rats ($n = 10$ /group), whose weight ranged from 550 to 650 g, were used for this study. Animals were acclimated to a reverse light/dark cycle for 2 weeks prior to the start of the experiment. Animals were placed on high fat diet (D-12492, Research Diets, New Brunswick, NJ) at 7 weeks of age. The study began at week 14 of high fat diet treatment and continued for an additional 23 days. At day 23, an oral glucose tolerance test (OGTT) was performed to study the effects of treatments on glucose tolerance. Prior to the glucose challenge, animals were fasted for 2 h and then given an oral glucose bolus (2 g/kg). Glucose measurements were taken via tail vein blood collection at 0, 30, 60, and 120 min after glucose challenge.

DGAT-1 Enzyme Assays. Insect cells (High 5) were transfected with recombinant baculovirus containing human DGAT-1 sequence and harvested after 48 h. Cells (1×10^{10}) were suspended in 500 mL of buffer A (50 mM Tris-HCl, pH 7.5, 100 mM NaCl, 1 mM EDTA, and protease inhibitors (complete protease inhibitor cocktail from Roche Diagnostics, catalog no. 11873580001)) at 4 °C. Cells were lysed by sonication (3 \times 30 s) and membranes isolated by centrifugation at 100000g for 60 min. Pellets were resuspended in 500 mL of buffer A plus 0.5% Triton X-100 and stirred for 30 min, sonicated (2 \times 30 s), and centrifuged at 100000g for 60 min. DGAT-1 containing pellets were then rinsed twice with small amounts of buffer A and homogenized in 300 mL of buffer A by sonication. Protein concentration was 9.85 mg/mL as determined by Bio-Rad protein assay reagents (catalog no. 500-00006). Aliquots were stored at –80 °C.

Rat DGAT-1 was also produced in High 5 insect cells and purified by the same procedures as described above. Protein concentration was 35.9 mg/mL as determined by Bio-Rad assay. Aliquots were stored at –80 °C.

(A) **Radioactive DGAT-1 Phospholipid (PL) FlashPlate Assay.** Human DGAT-1 activities were measured by radioactive PL-FlashPlate assays. Typically, 10 mM 1,2-dioleoyl-*sn*-glycerol (DAG) suspended in water containing 0.1% Triton X-100 was diluted to 0.5 mM with coating buffer purchased from PerkinElmer (catalog no. SMP900A). The diluted DAG solution was then added to 384-well PL-FlashPlates (PerkinElmer, catalog no. SMP 108) at 60 μ L per well and incubated at room temperature for 2 days. Plates were washed twice with buffer B (50 mM Tris-HCl, pH 7.5, 100 mM NaCl, and 0.05% deoxycholic acid). Test compounds at 0–2 mM in 100% DMSO were diluted 10-fold with buffer C (50 mM Tris-HCl, pH 7.5, 100 mM NaCl, and 0.01% BSA), and 20 μ L of solutions were added into the PL-FlashPlates. To each well was then added 15 μ L of 8.3 μ M palmitoyl-1-¹⁴C coenzyme A (PerkinElmer, catalog no. NEC-555) in buffer C followed by 15 μ L of human DGAT-1 enzyme solution (0.13 mg of total protein/mL) diluted in buffer A plus 0.2% Triton X-100. The reaction mixtures were incubated at 37 °C for 1 h and washed 3 times with buffer B to stop the reaction. Plates were sealed and read on a TopCount instrument from PerkinElmer.

Rat DGAT-1 was measured by the same procedure as described above except that the final enzyme concentration in the reaction mixture was 0.02 mg of total protein/mL.

(B) **Radioactive DGAT-1 TLC Assay.** DGAT-1 activity was also measured by a radioactive TLC method. This assay was used for comparing compound potency against DGAT-2 and ACAT. Typically, DGAT-1

(20 μ L, 0.13 mg of total protein/mL) in buffer A plus 0.2% Triton X-100 was incubated with 10 μ L of test compound solutions (0–600 μ M) in 20% DMSO in buffer C in Eppendorf tubes for 15 min on ice. DAG solution (50 μ L of 0.5 mM in coating buffer) was then added followed by 20 μ L of 8.3 μ M palmitoyl-1- 14 C coenzyme A in buffer C and the reaction mixture incubated at 37 $^{\circ}$ C for 1 h. The reaction was stopped by adding 0.3 mL of chloroform/methanol (2:1, v/v). The mixture was shaken for 5 min and centrifuged. The aqueous phase was discarded, and 100 μ L of the organic phase containing triglyceride product was spotted on TLC plates. Lipids were separated with a solvent system of petroleum ether/ether/acetic acid (80:20:1, v/v/v) for 35 min and plates analyzed on a phosphorimager after overnight exposure.

DGAT-2 Enzyme Assay. Sf9 insect cells were transfected with recombinant baculovirus containing DGAT-2 sequence and harvested after 48 h. Cells (4×10^9) were suspended in 230 mL of buffer A at 4 $^{\circ}$ C. Cells were lysed by sonication (3×30 s) and membranes isolated by centrifugation at 100000g for 60 min. DGAT-2 containing pellets were resuspended in 90 mL of buffer A and sonicated (1×30 s). Protein concentration was 6.29 mg/mL as determined by Bio-Rad assay, and aliquots were stored at –80 $^{\circ}$ C.

DGAT2 enzymatic activity was measured by radioactive TLC assay. DGAT-2 was diluted in 50 mM Tris-HCl, pH 7.5, 20 mM MgCl₂ plus 0.25 M sucrose to 0.313 mg/mL, and 20 μ L was incubated with 10 μ L of compound solutions (0–600 μ M) in 20% DMSO in 100 mM Tris-HCl, pH 7.5, 20 mM MgCl₂, and 0.125% BSA in Eppendorf tubes for 15 min on ice. DAG solution (50 μ L of 0.5 mM in coating buffer) was then added followed by 20 μ L of 8.3 μ M palmitoyl-1- 14 C coenzyme A in buffer C and the reaction mixture incubated at 37 $^{\circ}$ C for 5 min. The reaction was stopped, and lipids were analyzed as described above.

ACAT Enzyme Assay. HepG2 cells (2×10^8) containing a mixture of ACAT1 and ACAT2 were suspended in 10 mL of buffer A at 4 $^{\circ}$ C. Cells were lysed by sonication (3×30 s) and membranes isolated by centrifugation at 100000g for 60 min. ACAT containing pellets were resuspended in 5 mL of buffer A and sonicated (1×30 s). Protein concentration was 2.6 mg/mL as determined by Bio-Rad assay, and aliquots were stored at –80 $^{\circ}$ C.

ACAT activity was measured by radioactive TLC assay. ACAT solution was diluted in buffer A to 0.52 mg/mL, and 20 μ L was incubated with 10 μ L of compound solutions (0–600 μ M) in 20% DMSO in buffer C for 15 min on ice followed by 70 μ L of 2.37 μ M palmitoyl-1- 14 C coenzyme A in buffer C. The reaction mixture incubated at 37 $^{\circ}$ C for 1 h. For lipid analysis on TLC, a solvent system of petroleum ether/ether/acetic acid (90:10:1, v/v/v) was used.

■ ASSOCIATED CONTENT

S Supporting Information. Results of radiolabeled binding assay of compound **29** and effect of compound **29** on insulin levels. This material is available free of charge via the Internet at <http://pubs.acs.org>.

■ AUTHOR INFORMATION

Corresponding Author

*Phone: (973) 235-3240. Fax: (973) 235-6263. E-mail: yimin.qian@roche.com.

■ ACKNOWLEDGMENT

We thank Dr. Paul Gillespie, Dr. Robert Goodnow, Dr. Jianping Cai, and Dr. Christophe Michoud for their DGAT-1 hit identification work, Gino Sasso and Theresa Burchfield for 1 H NMR help, Vance Bell for mass spectrometry experiments, and Dr. Ramakanth Sarabu for helpful discussions and reading of the manuscript.

■ ABBREVIATIONS USED

DGAT-1, diacylglycerol acyltransferase-1; hERG, human ether-a-go-go-related gene; DIO, diet induced obesity; OGTT, oral glucose tolerance test; GLP-1, glucagon-like peptide-1; PYY, peptide YY; PyBroP, bromotripyrrolidinophosphonium hexafluorophosphate; BOP, (benzotriazol-1-yloxy)tris(dimethylamino)-phosphonium hexafluorophosphate; PdCl₂(dppf), dichloro[1,1'-bis(diphenylphosphino)ferrocene]palladium(II)

■ REFERENCES

- (1) Cases, S.; Smith, S. J.; Zheng, Y-W; Myers, H. M.; Lear, S. R.; Sande, E.; Novak, S.; Collins, C.; Welch, C. B.; Lusis, A. J.; Erickson, S. K.; Farese, R. V., Jr. Identification of a gene encoding an acyl CoA: diacylglycerol acyltransferase, a key enzyme in triacylglycerol synthesis. *Proc. Natl. Acad. Sci. U.S.A.* **1998**, *95*, 13018–13023.
- (2) Cases, S.; Stone, S. J.; Zhou, P.; Yen, E.; Tow, B.; Lardizabal, K. D.; Voelker, T.; Farese, R. V., Jr. Cloning of DGAT2, a second mammalian diacylglycerol acyltransferase, and related family members. *J. Biol. Chem.* **2001**, *276*, 38870–38876.
- (3) Yen, C. E.; Stone, S. J.; Koliwad, D.; Harris, C.; Farese, R. V., Jr. DGAT enzymes and triacylglycerol biosynthesis. *J. Lipid Res.* **2008**, *49*, 2283–2301.
- (4) Smith, S. J.; Cases, S.; Jensen, D. R.; Chen, H. C.; Sande, E.; Tow, B.; Sanan, D. A.; Raber, J.; Eckel, R. H.; Farese, R. V., Jr. Obesity resistance and multiple mechanisms of triglyceride synthesis in mice lacking DGAT. *Nat. Genet.* **2000**, *25*, 87–90.
- (5) Chen, H. C.; Smith, S. J.; Ladha, Z.; Jensen, D. R.; Ferreira, L. D.; Pulawa, L. K.; McGuire, J. G.; Pitas, R. E.; Eckel, R. H.; Farese, R. V., Jr. Increased insulin and leptin sensitivity in mice lacking acyl CoA: diacylglycerol acyltransferase 1. *J. Clin. Invest.* **2002**, *109*, 1049–1055.
- (6) Stone, S. J.; Myers, H. M.; Watkins, S. M.; Brown, B. E.; Feingold, K. R.; Elias, P. M.; Farese, R. V., Jr. Lipopenia and skin barrier abnormalities in DGAT2-deficient mice. *J. Biol. Chem.* **2004**, *279*, 11767–11776.
- (7) Lee, B.; Fast, A. M.; Zhu, J.; Cheng, J.; Buhman, K. K. Intestine-specific expression of acyl CoA:diacylglycerol acyltransferase 1 reverses resistance to diet-induced hepatic steatosis and obesity in Dgat1 $^{-/-}$ mice. *J. Lipid Res.* **2010**, *51*, 1770–1780.
- (8) King, A. J.; Judd, A. S.; Souers, A. J. Inhibitors of diacylglycerol acyltransferase: a review of 2008 patents. *Expert Opin. Ther. Patents* **2010**, *20*, 19–29.
- (9) (a) Birch, A. M.; Buckett, L. K.; Turnbull, A. V. DGAT1 inhibitors as anti-obesity and anti-diabetic agents. *Curr. Opin. Drug Discovery Dev.* **2010**, *13*, 489–496. (b) Matsuda, D.; Tomoda, H. Triazolo Compounds Useful as Diacylglycerol Acyltransferase1 Inhibitor-WO2009126624. *Expert Opin. Ther. Pat.* **2010**, *20*, 1097–1102. (c) Fox, B. M.; Iio, K.; Li, K.; Choi, R.; Inaba, T.; Jackson, S.; Sagawa, S.; Shan, B.; Tanaka, M.; Yoshida, A.; Kayser, F. Discovery of pyrrolopyridazines as novel DGAT1 inhibitors. *Bioorg. Med. Chem. Lett.* **2010**, *20*, 6030–6033.
- (10) (a) Nakada, Y.; Aicher, T. D.; Le Huerou, Y.; Turner, T.; Pratt, S. A.; Gonzales, S. S.; Boyd, S. A.; Miki, H.; Yamamoto, T.; Yamaguchi, H.; Kato, K.; Kitamura, S. Novel acyl coenzyme A (CoA):diacylglycerol acyltransferase-1 inhibitors: synthesis and biological activities of diacyl-ethylenediamine derivatives. *Bioorg. Med. Chem.* **2010**, *18*, 2785–2795. (b) Yamamoto, T.; Yamaguchi, H.; Miki, H.; Shimada, M.; Nakada, Y.; Ogino, M.; Asano, K.; Aoki, K.; Tamura, N.; Masago, M.; Kato, K. Coenzyme A:diacylglycerol acyltransferase I inhibitor ameliorates obesity, liver steatosis, and lipid metabolism abnormality in KKA Y mice fed high-fat or high-carbohydrate diets. *Eur. J. Pharmacol.* **2010**, *640*, 243–249.
- (11) Smith, R.; Campbell, A.-M.; Coish, P.; Dai, M.; Jenkins, S.; Lowe, D.; O'Connor, S.; Su, N.; Wang, G.; Zhang, M.; Zhu, L. Preparation of Benzazolyaminobiphenyloxoalkanoates for the Treatment of Obesity. Patent US 2004/0224997, 2004.

- (12) (a) Fox, B. M.; Furukawa, N.; Hao, X.; Iio, K.; Inaba, T.; Jackson, S. M.; Kayser, F.; Labelle, M.; Li, K.; Matsui, T.; McMinn, D. L.; Ogawa, N.; Rubenstein, S. M.; Sagawa, S.; Sugimoto, K.; Suzuki, M.; Tanaka, M.; Ye, G.; Yoshida, A.; Zhang, J. A Preparation of Fused Bicyclic Nitrogen-Containing Heterocycles. Patent WO 2004/047755, 2004. (b) Fox, B. M.; Iio, K.; Li, K.; Inaba, T.; Labelle, M.; Rubenstein, S.; Ye, G.; Zhang, J.; Jackson, S.; Choi, R.; Sagawa, S.; Shan, B.; Tanaka, M.; Yoshida, A.; Kayser, F. Discovery of Pyrimidooxazines as Novel DGAT1 Inhibitors Efficacious in a Mouse Diet-Induced Obesity Model. Presented at the 32nd Annual National Medicinal Chemistry Symposium, Minneapolis, MN, June 6–9, 2010.
- (13) Zhao, G.; Souers, A. J.; Voorbach, M.; Falls, H. D.; Droz, B.; Brodjan, S.; Lau, Y. Y.; Iyengar, R. R.; Gao, J.; Judd, A. S.; Wagaw, S. H.; Ravn, M. M.; Engstrom, K. M.; Lynch, J. K.; Mulhern, M. M.; Freeman, J.; Dayton, B. D.; Wang, X.; Grihalde, N.; Fry, D.; Beno, D. W. A.; Marsh, K. C.; Su, Z.; Diaz, G. J.; Collins, C. A.; Sham, H.; Reilly, R. M.; Brune, M. E.; Kym, P. R. Validation of diacyl glycerol acyltransferase I as a novel target for the treatment of obesity and dyslipidemia using a potent and selective small molecule inhibitor. *J. Med. Chem.* **2008**, *51*, 380–383.
- (14) Birch, A. M.; Birtles, S.; Buckett, L. K.; Kemmitt, P. D.; Smith, G. J.; Smith, T. J. D.; Turnbull, A. V.; Wang, S. J. Y. Discovery of a potent, selective, and orally efficacious pyrimidinoxazinyl bicyclooctaneacetic acid diacylglycerol acyltransferase-1 inhibitor. *J. Med. Chem.* **2009**, *52*, 1558–1568.
- (15) Dow, R. L.; Li, J.-C.; Parel, L.; Perreault, C.; Munchhof, M. J.; Piotrowski, D. W.; Gibbs, E. M.; Zavadski, W. J.; Manion, T. B.; Treadway, J. L.; La Perle, J. L. Discovery and Preclinical Pharmacology of PF-04620110: A Selective Inhibitor of DGAT-1 for the Treatment of Type-2 Diabetes. Presented at the 239th National Meeting of the American Chemical Society, San Francisco, CA, March 21–25, 2010; MEDI-315.
- (16) (a) Wertheimer, S. J.; Bolin, D.; Erickson, S.; Conde-Knape, K.; Belunis, C.; Konkar, A.; Taub, R.; Rondinone, C. M. Fatty acid modulators for the treatment of diabetes. *Drug Discovery Today: Ther. Strategies* **2007**, *4* (2), 129–135. (b) Bolin, D. R.; Cheung, A. W.-H.; Firooznia, F.; Hamilton, M. M.; Li, S.; McDermott, L. A.; Qian, Y.; Yun, W. Diacylglycerol Acyltransferase Inhibitors. Patent US 7,714,126, May 11, 2010. (c) Bolin, D. R.; Michoud, C. Inhibitors of Diacylglycerol Acyltransferase (DGAT). WO 2006/082010, 2006.
- (17) Yun, W.; Bolin, D. R.; Li, S.; Ahmad, M.; Wertheimer, S. J.; Conde-Knape, K.; Chen, Y.; Kazmer, S. Discovery and Optimization of Oxazole Based Diacylglycerol Acyltransferase-1 Inhibitor for the Treatment of Obesity. Presented at the 237th National Meeting of the American Chemical Society, Salt Lake City, UT, March 22–26, 2009; MEDI-256.
- (18) Zhu, B.; Jia, Z.; Zhang, P.; Su, T.; Huang, W.; Goldman, E.; Tumas, D.; Kadambi, V.; Eddy, P.; Sinha, U.; Scarborough, R. M.; Song, Y. Inhibitory effects of carboxylic acid group on hERG binding. *Bioorg. Med. Chem. Lett.* **2006**, *16*, 5507–5512.
- (19) Redfern, W. S.; Carlsson, L.; Davis, A. S.; Lynch, W. G.; MacKenzie, I.; Palethorpe, S.; Siegl, P. K. S.; Strang, I.; Sullivan, A. T.; Wallis, R.; Camm, A. J.; Hammond, T. G. Relationships between preclinical cardiac electrophysiology, clinical QT interval prolongation and torsade de pointes for a broad range of drugs: evidence for a provisional safety margin in drug development. *Cardiovasc. Res.* **2003**, *58*, 32–45.
- (20) Lagrutta, A. A.; Trepakova, E. S.; Salata, J. J. The hERG channel and risk of drug-acquired cardiac arrhythmia: an overview. *Curr. Top. Med. Chem.* **2008**, *8*, 1102–1112.
- (21) Okawa, M.; Fujii, K.; Ohbuchi, K.; Okumoto, M.; Aragane, K.; Sato, H.; Tamai, Y.; Seo, T.; Itoh, Y.; Yoshimoto, R. Role of MGAT2 and DGAT1 in the release of gut peptides after triglyceride ingestion. *Biochem. Biophys. Res. Commun.* **2009**, *390*, 377–381.
- (22) Murphy, K. G.; Bloom, S. R. Gut hormones and the regulation of energy homeostasis. *Nature* **2006**, *444*, 854–859.
- (23) Larsen, P. J. Mechanisms behind GLP-1 induced weight loss. *Br. J. Diabetes Vasc. Dis.* **2008**, *8*, S34–S41.
- (24) Ogawa, N.; Okuma, C.; Furukawa, N. Anorectic Compounds. Patent WO2005/072740, 2005.
- (25) Guo, L.; Guthrie, H. Automated electrophysiology in the preclinical evaluation of drugs for potential QT prolongation. *J. Pharmacol. Toxicol. Methods* **2005**, *52*, 123–135.